Received: 23 August 2021 | Revised: 21 February 2022 | Accepted: 23 February 2022

DOI: 10.1002/cne.25314

RESEARCH ARTICLE

JCN RESEARCH IN SYSTEMS NEUROSCIENCE THE JOURNAL OF COMPARATIVE NEUROLOGY WILEY

Nicotinic acetylcholine receptors in a songbird brain

Norman Chinweike Asogwa[1] | Noriyuki Toji[2] | Ziwei He[1] | Chengru Shao[1] | Yukino Shibata[1] | Shoji Tatsumoto[3] | Hiroe Ishikawa[3] | Yasuhiro Go[3,4,5] | Kazuhiro Wada[1,2]

[1]Graduate School of Life Science, Hokkaido University, Sapporo, Japan

[2]Faculty of Science, Hokkaido University, Sapporo, Japan

[3]Cognitive Genomics Research Group, Exploratory Research Center on Life and Living Systems, National Institutes of Natural Sciences, Okazaki, Japan

[4]School of Life Science, SOKENDAI (The Graduate University for Advanced Studies), Okazaki, Japan

[5]Department of Physiological Sciences, National Institute for Physiological Sciences, Okazaki, Japan

Correspondence
Kazuhiro Wada, Faculty of Science, Hokkaido University, Room 910, Building No.5, North 10, West 8, Kita-ku, Sapporo, Hokkaido, 060–0810, Japan.
Email: wada@sci.hokudai.ac.jp

Norman Chinweike Asogwa and Noriyuki Toji contributed equally to this study.

Funding information
MEXT/JSPS KAKENHI, Grant/Award Numbers: 4903-JP17H06380, JP19H04888, JP21H02456, JP21K18265; Takeda Science Foundation; JASSO Follow-up Research Fellowship, Grant/Award Number: 153033

Abstract

Nicotinic acetylcholine receptors (nAChRs) are ligand-gated ion channels that mediate fast synaptic transmission and cell signaling, which contribute to learning, memory, and the execution of motor skills. Birdsong is a complex learned motor skill in songbirds. Although the existence of 15 nAChR subunits has been predicted in the avian genome, their expression patterns and potential contributions to song learning and production have not been comprehensively investigated. Here, we cloned all the 15 nAChR subunits (ChrnA1–10, B2–4, D, and G) from the zebra finch brain and investigated the mRNA expression patterns in the neural pathways responsible for the learning and production of birdsong during a critical period of song learning. Although there were no detectable hybridization signals for ChrnA1, A6, A9, and A10, the other 11 nAChR subunits were uniquely expressed in one or more major subdivisions in the song nuclei of the songbird brain. Of these 11 subunits, ChrnA3–5, A7, and B2 were differentially regulated in the song nuclei compared with the surrounding anatomically related regions. ChrnA5 was upregulated during the critical period of song learning in the lateral magnocellular nucleus of the anterior nidopallium. Furthermore, single-cell RNA sequencing revealed ChrnA7 and B2 to be the major subunits expressed in neurons of the vocal motor nuclei HVC and robust nucleus of the arcopallium, indicating the potential existence of ChrnA7-homomeric and ChrnB2-heteromeric nAChRs in limited cell populations. These results suggest that relatively limited types of nAChR subunits provide functional contributions to song learning and production in songbirds.

KEYWORDS
acetylcholine, nicotinic receptors, sensorimotor learning, vocal learning, zebra finch

Abbreviations: A, arcopallium; AA, anterior arcopallium; AD, dorsal arcopallium; AI, intermediate arcopallium; AId, dorsal part of AI; AIv, ventral part of AI; AMVi, intermediate part of the medial ventral arcopallium; AP, posterior arcopallium; Area X, striatum song nucleus area X; B, nucleus basorostralis; Cb, cerebellum; CMM, caudomedial mesopallium; DLM, dorsolateral nucleus of medial thalamus; DM, dorsal medial nucleus of the midbrain; dn, deep nuclei of the cerebellum; E, entopallium; g, granular layer of the cerebellar cortex; Gp, globus pallidus; H, hyperpallium; Hp, hippocampus; HVC, acronym as proper name used for the song nucleus; IPc, nucleus isthmi pars parvocellularis; L, field L subdivision of nidopallium; LMAN, lateral magnocellular nucleus of the anterior nidopallium; M, mesopallium; m, molecular layer of the cerebellar cortex; MLd, nucleus mesencephalicus lateralis pars dorsalis; MMAN, medial magnocellular nucleus of the anterior nidopallium; N, nidopallium; NCM, caudomedial nidopallium; P, pallidum; p, Purkinje cell layer of the cerebellar cortex; Pt, nucleus pretectalis; RA, robust nucleus of the arcopallium; Rt, nucleus rotundus; SP, nucleus subpretectalis; Spl, nucleus spiriformis lateralis; Str, striatum; TeO, tectum opticum; Tha, thalamus; TnA, nucleus taenia; w, white matter layer in the cerebellum

1 | INTRODUCTION

In the CNS, acetylcholine receptors (AChRs) mediate acetylcholine (ACh) function in the arousal-related enhancement of sensory processing (Fu et al., 2014; Herrero et al., 2008; Shea et al., 2010), cognition and memory (Anagnostaras et al., 2003; Hasselmo, 2006; Wallace & Bertrand, 2013), motor skill acquisition (Conner et al., 2003; H. Q. Li & Spitzer, 2020; Thouvarecq et al., 2001), and selective attention (Noudoost & Moore, 2011; Parikh et al., 2007; Sarter et al., 1999). These AChR-mediated physiological processes are likely shared among vertebrate species because of the high conservation of AChR protein sequences and their related signaling pathways (Dajas-Bailador & Wonnacott, 2004; Gotti & Clementi, 2004; Pedersen et al., 2019). However, except for the extensively studied species of mammals, fundamental knowledge about the expression of AChRs in the CNS is limited in vertebrates, including avian species.

AChRs comprise two major classes: muscarinic and nicotinic receptors (Gotti & Clementi, 2004; Kruse et al., 2014). Nicotinic AChRs (nAChRs) are ligand-gated ion channels that are permeable to Na^+, K^+, and Ca^{2+} ions. Hence, nAChRs mediate not only fast synaptic transmission but also intracellular signaling via Ca^{2+}-dependent signaling machinery (Dajas-Bailador & Wonnacott, 2004; Gotti et al., 2009; Wonnacott, 1997; M. Zoli et al., 2018). Functional nAChRs exist in either homo- or hetero-pentameric configurations formed from α subunits (ChrnAs) as the ligand binding subunits and β subunits (ChrnBs) as structural subunits (Couturier et al., 1990; Gotti et al., 2009; N. Le Novere et al., 2002; M. Zoli et al., 2015). To date, the existence of 15 nAChR subunits (ChrnA1–10, B2–4, D, and G) is predicted in the genome of avian species. In comparison, mammals do not retain ChrnA8 but express two additional subunits, ChrnB1 and ChrnE. Although the number and types of nAChR subunits are not perfectly conserved between avian and mammalian species, the phylogenetic relationship between homologous subunit genes is highly conserved (Lovell et al., 2020; Pedersen et al., 2019; Sargent, 1993; Wada et al., 1988) (Figure 1a).

Based on their pharmacological and structural properties, nAChR subunits are divided into three major functional groups: muscle subunits (ChrnA1, B1, D, E, and G), standard neuronal subunits that form heteromeric receptors with pairwise α (ChrnA2–6) and β (ChrnB2–4) subunit combinations, and other neuronal subunits (ChrnA7–10) that can form homomeric nAChRs (Gotti et al., 2009; M. Zoli et al., 2015). These different combinations are associated with specific physiological and developmental features (Gotti et al., 2009; Role & Berg, 1996; Zoli et al., 1995). Some neuronal nAChR subunits are selectively expressed in specific subregions of the CNS in vertebrates, including mammals (Dineley-Miller & Patrick, 1992; Han et al., 2000; Wada et al., 1988; Winzer-Serhan & Leslie, 1997; Zoli et al., 1995) and birds (Halvorsen & Berg, 1990; Lovell et al., 2018; Morris et al., 1990; Whiting et al., 1991). However, at the single-cell level, the combinations of nAChR subunits that are coexpressed in the CNS have not yet been fully elucidated.

Oscine songbirds learn birdsong, a complex vocal skill, during a critical period that comprises the sensory and sensorimotor learning phases (Brenowitz & Beecher, 2005; Doupe & Kuhl, 1999; Marler & Slabbekoorn, 2004). During the sensory learning phase, a juvenile bird listens to and memorizes a copy of the tutor song, while during the sensorimotor learning phase, the pupil bird practices singing repeatedly and refines its vocal outputs to mimic the memorized tutor song model through auditory feedback. Song acquisition is shaped by singing subsong, plastic song, and crystallized song. The learning and production of birdsong are controlled by specialized neural circuits known as song pathways (Figure 1b). These song pathways are organized into two anatomically and functionally distinct neural circuits called the anterior pathway (AFP) and vocal motor pathway (VMP), with interconnecting song nuclei. The AFP consists of a pallial–basal ganglia–thalamic connection with three song nuclei: the lateral magnocellular nucleus of the anterior nidopallium (LMAN), nucleus Area X in the striatum, and anterior part of the medial nucleus of the dorsolateral thalamus (aDLM, the part of DLM that receives afferent input from Area X and sends output projection to LMAN) (Luo et al., 2001). The VMP comprises the HVC (acronym as proper name) and robust nucleus of the arcopallium (RA). Although the VMP participates in song production, the AFP is not required for singing but is a crucial neural circuit for song learning and maintenance by generating vocal fluctuations (Andalman & Fee, 2009; Bottjer et al., 1984; Brainard & Doupe, 2000; Kao et al., 2005; Nottebohm et al., 1976; Scharff & Nottebohm, 1991).

In songbirds, ACh and associated enzymes such as acetylcholinesterase (AChE) and choline acetyltransferase (ChAT) exist in several song nuclei (Ryan & Arnold, 1981; Sakaguchi & Saito, 1989; Zuschratter & Scheich, 1990). Song nucleus HVC receives cholinergic afferents from the ventral pallidum of the basal forebrain, a brain region homologous to the nucleus basalis of Meynert in mammals (R. Li & Sakaguchi, 1997; Reiner et al., 2004). In addition, the concentration of ACh increases in the song nuclei HVC, RA, and LMAN of male zebra finches during the early critical period of song learning (Sakaguchi & Saito, 1989). Similarly, AChE is highly enriched in the song nuclei HVC, RA, and LMAN during this critical period (Ryan & Arnold, 1981; Sadananda, 2004; Sakaguchi & Saito, 1991). These findings suggest the expression of AChRs in the song nuclei that mediates cholinergic functions during song learning and production. Our previous investigation revealed developmental regulation and inter- and intraspecific differences in the expression of muscarinic AChR subunits (mAChRs) in the song pathways (Asogwa et al., 2018). In contrast to mAChRs, only a limited number of nAChR subunits have been reported to be expressed in the songbird brain (Lovell et al., 2008, 2018; Watson et al., 1988). ZEBrA, the online public repository of gene expression in the zebra finch brain (http://www.zebrafinchatlas.org/), currently provides in situ hybridization information for nAChR subunits ChrnA3–5, A7, B2, and B3 (Lovell et al., 2020). However, the precise number of nAChR subunits involved and their expression levels and patterns, particularly in the song nuclei, during song development have not been fully investigated.

Here, we cloned 15 nAChR subunits from the zebra finch brain; however, no detectable signal was obtained in the brain sections by in situ hybridization for four subunits. The remaining 11 subunits were expressed to varying levels in at least one brain subdivision

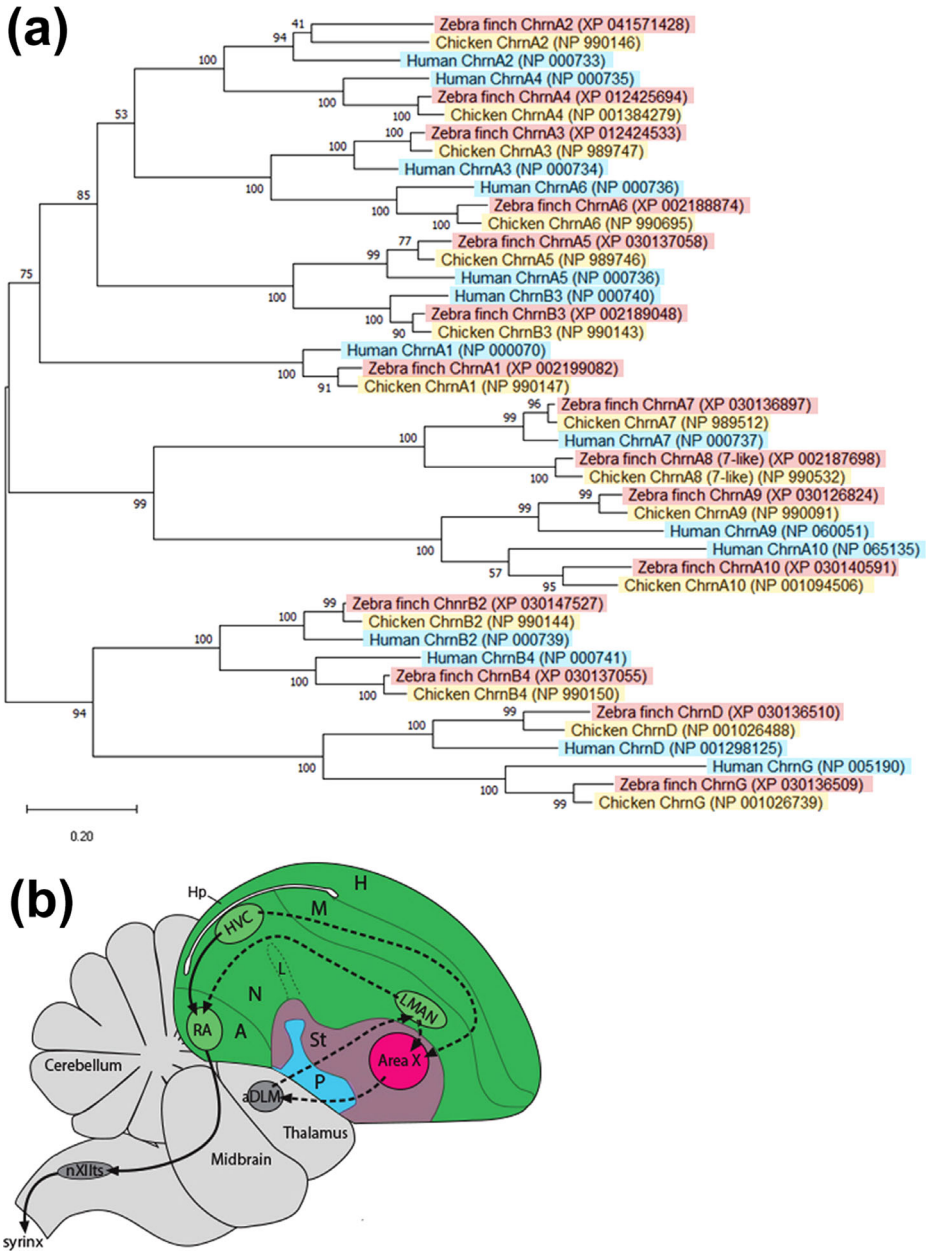

FIGURE 1 Phylogram of nicotinic acetylcholine receptor subunits and brain diagram of the neural circuits for song learning and production. (a) Phylogenetic relationship of nicotinic acetylcholine receptor (nAChR) subunits in the zebra finch, chicken, and human, generated with full-length protein-coding sequences using Molecular Evolutionary Genetics Analysis software (https://www.megasoftware.net/). Local bootstrap probabilities from the maximum-likelihood analysis are shown for branches below the terminals. All subunit types show closer homologies to each other across species than they do to different receptor types within species. (b) The vocal motor circuit and the anterior forebrain pathway (pallial–basal ganglia–thalamic loop circuit) are represented as solid and dotted black lines, respectively. A, arcopallium; Area X, Area X of the striatum; aDLM, anterior dorsal lateral nucleus of the medial thalamus; H, hyperpallium; Hp, hippocampus; HVC (proper name); L, field L; LMAN, lateral magnocellular nucleus of the anterior nidopallium; M, mesopallium; N, nidopallium; nXIIts, the tracheosyringeal part of the 12th cranial nerve nuclei; RA, robust nucleus of the arcopallium; P, pallidum; St, Striatum

(pallium, hippocampus, subpallium, midbrain, or cerebellum). Specifically, the expression of ChrnA3–5, A7, and B2 revealed unique specializations in one or more song nuclei. In addition, the single-cell transcriptional analysis revealed the potential existence of ChrnA7-homomeric and ChrnB2-heteromeric nAChRs in the vocal motor nuclei.

2 | MATERIALS AND METHODS

2.1 | Animals

Male zebra finches (*Taeniopygia guttata*) were used for this study at the three stages of song development: subsong (30–45 posthatching day

[phd], $n = 6$), plastic song (50–65 phd, $n = 6$), and the crystallized song (>120 phd, $n = 6$). Because of the limited number of brain sections available in one of six brains, only five birds at the subsong stage were utilized for in situ hybridization with ChrnA4, A5, and A10 probes. For that same reason, in situ hybridization for ChrnA4 and A10 probes was performed with five birds at the plastic song stage. The birds were used from our breeding colonies at Hokkaido University, Sapporo, Japan. Photoperiod was maintained at 13 h light/11 h dark cycle with free access to food and water. Song developmental stages were confirmed by the probability density distribution of syllable duration in songs (Aronov et al., 2011). All animal-based procedures complied with the regulations of the Committee on Animal Experiments of Hokkaido University. These regulations are requirements of the National Regulations for Animal Welfare in Japan (Law for the Humane Treatment and Management of Animals, partial amendment number No. 105, 2011).

2.2 | Reverse transcription PCR and cloning of nAChR subunits

Attempts were made to clone, from the zebra finch brain, all 15 nAChR subunits identified or predicted in birds (Pedersen et al., 2019; Sargent, 1993). The ChrnA7-like subunit in the National Centre for Biotechnology Information (NCBI, accession no. XM_002187662) was labeled as ChrnA8. Reverse transcription PCR (RT-PCR) was performed on total RNA collected from adult male zebra finch brains before light-on in the morning. Total RNA was extracted by TRIzol Reagent (Thermo Fisher, Waltham, MA, USA), treated with DNaseI to digest contamination from genome DNA, and transcribed to complementary DNA (cDNA) using Superscript Reverse Transcriptase (Thermo Fisher) with oligo(dT) primers. In the first attempt to clone the targeted subunits, we designed PCR oligo-primers to target protein regions that are conserved between mammals, birds, reptiles, and amphibians (Table 1). When the initial cloning failed, we used putative mRNA sequences predicted by the NCBI for primer design. Partial DNA fragment of each targeted nAChR subunit was amplified by PCR (Ex Taq polymerase, Takara Bio, Shiga, Japan) using the synthesized cDNA template and cloned into pGEM-T easy plasmids (Promega) based on a previous method (Asogwa et al., 2018; Wada et al., 2004). The cloned cDNA fragments were verified by DNA sequencing. The sequence identities of cloned cDNA fragments and their predicted amino acids were authenticated by comparison with the transcripts of nAChR subunits in the zebra finch, chicken, and human in the NCBI, using Nucleotide and Protein BLASTs. The cloned partial cDNA sequences of 15 nAChR subunits were assigned in GenBank with accession numbers OL679454–OL679467 and OM201170 (Table 1).

2.3 | Radioisotope in situ hybridization and quantification of mRNA expression

Brain tissues were sampled from birds in dark, silent, and nonsinging conditions. To ensure that mRNA expression was not due to singing or hearing songs, the birds were kept in a sound-attenuation box under these conditions for at least 10 h prior to euthanasia and sacrifice. Brain tissues were put in plastic molds with tissue-compounding medium (Tissue-Tek; Sakura Finetek, Torrance, CA, USA) and immediately transferred onto crushed dry ice. Subsequently, they were stored at −80°C until sectioning. The brain tissues were sectioned at 12 μm thickness on the sagittal plane and mounted on silane-coated slides. The radioisotope in situ hybridization and quantification of expressed mRNA levels were conducted according to previous studies (Asogwa et al., 2018). Using specific T7 or SP6 RNA polymerases (Roche, Basel, Switzerland) to the inserted sense-/antisense direction of nAChR subunits, ^{35}S-labeled riboprobes were synthesized from the T7 or SP6 promoter sites of pGEM-T. Fresh frozen brain sections were fixed in 3% paraformaldehyde/1× phosphate-buffered saline (PBS, pH 7.0), washed three times in 1× PBS, acetylated, washed three times in 2× SSPE, dehydrated in ascending ethanol concentrations (50%, 70%, 90%, and 100%), and then air-dried. Each Riboprobe (10^6 cpm) was mixed with 150 μl of hybridization buffer (50% formamide; 10% dextran sulfate; 1× Denhart's solution; 12 mM EDTA, pH 8.0; 10 mM Tris–HCl, pH 8.0; 30 mM NaCl; 0.5 μg/μl yeast tRNA; and 10 mM dithiothreitol. Hybridization was performed in an oil bath for 14 h at 65°C. Slides were next washed stepwise in two changes of chloroform, in 2× SSPE/0.1% 2β-mercaptoethanol for 30 min, in 50% formamide/0.1% 2β-mercaptoethanol for 60 min, twice in 2× SSPE/0.1% 2β-mercaptoethanol for 30 min each, and twice in 0.1× SSPE/0.1% 2β-mercaptoethanol for 15 min each. For ChrnA2, because of the high %GC contents (65% GC) of its probe, hybridization and washing temperatures were set at 68.5°C. The slides were dehydrated in ascending ethanol concentrations (50%, 70%, 90%, and 100%), air-dried, and exposed to BioMax MR Films (Kodak, Waltham, MA, USA) for 4–5 days before development. mRNA signals were quantified from X-ray films by digitally scanning them under a microscope (Z16 Apo; Leica, Buffalo Grove, IL, USA) that was connected to a CCD camera (DFC490; Leica), with Leica Application Suite, version 3.3.0 (Leica). Light and camera settings were maintained constant for all images to avoid biased comparisons. Images were converted to a 256-gray scale. mRNA expression levels were quantified as mean pixel intensities using Adobe Photoshop (CS2, Adobe Systems, San Jose, CA, RRID: SCR_014199). After X-ray film exposure, brain slides were Nissl-stained with Cresyl violet acetate solution (Sigma, St Louis, MO, USA) to aid visual evaluation of anatomical subregions. For the figure presenting mRNA expression in the brain, images of in situ hybridization taken in sagittal sections were oriented with the rostral side to the right and the dorsal side upward, and the black-and-white negatives were inverted, so that white represents mRNA signal. Based on careful comparison of in situ hybridization images taken from 10 birds, we were able to distinguish real signals from artifacts. Apparent artifacts from in situ hybridization images were identified as shown in Figures 2–4, and were removed in Photoshop using The Spot Healing Brush Tool function.

2.4 | Single-cell RNA sequencing

The brain of an adult male zebra finch was used for single-cell RNA sequencing (scRNA-seq) experiment. The bird was placed in a

TABLE 1 Cloned partial complementary DNA (cDNA) information of nicotinic acetylcholine receptors (nAChR) subunits in this study[1]

Cloned subunits in this study	Forward primer	Reverse primer	Cloned fragment length (bp)	Accession No. of cloned subunits in this study	Accession No. of zebra finch predicted nAChR mRNAs	Position at protein coding sequence	Similarity to zebra finch predicted nAChR proteins	Similarity to chicken nAChR proteins	Similarity to human nAChR proteins
ChrnA1	5′-AATGGACAGACG TCAACCTC-3′	5′-CTGGAGGT GGAGGGAATCA-3′	592	OL679454	XM_002199046	86-282a.a./ 457a.a.	99% to XP_ 002199082	97% to NP_ 990147	89% to NP_ 000070
ChrnA2	5′-ACATCACCTTC TACTTCGTC-3′	5′-CGATGATGAAGA TCCAGAGG-3′	834	OL679455	XM_041715494	227-503a.a./ 522a.a.	100% to XP_ 041571428	73% to NP_ 990146	67% to NP_ 000733
ChrnA3	5′-AGTTGGGGA TTTCCAGGTTG-3′	5′-GTTCCTAGAAT ACATACCAGG-3′	1,051	OL679456	XM_012569079	126-474a.a./ 496a.a.	100% to XP_ 012424533	96% to NP_ 989747	87% to NP_ 00073
ChrnA4	5′-TGATGACCA CCAATGTGTGG-3′	5′-GCATGGACT CAATGAGCTTC-3′	842	OL679457	XM_012570240	84-363a.a./ 624a.a.	100% to XP_ 012425694	98% to NP_ 001384279	91% to NP_ 000735
ChrnA5	5′-TGGGTTCGT CCAGTGGAAC-3′	5′-GTGCAGAAATA TCTTGCGAAC-3′	854	OL679458	XM_030281197	45-328a.a./ 445a.a.	100% to XP_ 030137058	99% to NP_ 989746	92% to NP_ 000736
ChrnA6	5′-CAAACTGCG ATGGGATCCC-3′	5′-CTCTGTCTA TCACCATAGCTA-3′	1,038	OL679459	XM_002188838	125-460a.a./ 493a.a.	99% to XP_ 002188874	93% to NP_ 990695	80% to NP_ 004189
ChrnA7	5′-CTGCAAGGAGA GTTCCAAAG-3′	5′-GAAGGCCAT CAAGCAGAGC-3′	1,326	OL679460	XM_030281037	28-468a.a./ 502a.a.	100% to XP_ 030136897	98% to NP_ 989512	91% to NP_ 000737
ChrnA8 (7-like)	5′-GCTGCTTGT GGCTGAGATC-3′	5′-CAAACTTCCAC TCACTGCAG-3′	563	OL679461	XM_002187662	285-471a.a./ 511a.a.	99% to XP_ 002187698	86% to NP_ 990532	N/A
ChrnA9	5′-TATGCTCACAT GCTGTTTAATG-3′	5′-GAATCTCCCATT CCACATCTT-3′	486	OL679462	XM_030270964	6-166a.a./ 448a.a.	100% to XP_ 030126824	98% to NP_ 990091	91% to NP_ 060051
ChrnA10	5′-TTCGTGGAGA ACGTGGAGTG-3′	5′-TGATCATGGTC ATGGTGGCG-3′	303	OM201170	XM_030284731	203–302a.a./ 456a.a.	100% to XP_ 030140591	97% to NP_ 001094506	83% to NP_ 065135
ChrnB2	5′-AGCGGGAGCA GATCATGAC-3′	5′-CGCTGGTGACG ATGGAGAA-3′	694	OL679463	XM_030291667	72-302a.a./ 491a.a.	99% to XP_ 030147527	99% to NP_ 990144	98% to NP_ 000739
ChrnB3	5′-TTACCATCC CATGGCACCC-3′	5′-CAAAGTGTTG TTCAGCCACAT-3′	354	OL679464	XM_002189012	331-448a.a./ 455a.a.	99% to XP_ 002189048	91% to NP_ 990143	79% to NP_ 000740
ChrnB4	5′-GGAAGCATG GCAGCAGATG-3′	5′-CTGGTAACT ATTGAGAAGGTC-3′	730	OL679465	XM_030281195	26-298a.a. (spliced out 83–120a.a.)/489a.a.	100% to XP_ 030137055	99% to NP_ 990150	89% to NP_ 000741
ChrnD	5′-ATAGTCCTGGA GAACAACAATG-3′	5′-GCTTGTTCTC CTCCCGGTA-3′	1169	OL679466	XM_030280650	121-509a.a./ 518a.a.	99% to XP_ 030136510	85% to NP_ 001026488	67% to NP_ 001298125
ChrnG	5′-ATCTCTGCC ATGGCTGTGC-3′	5′-GCCTGGTTG AAGTGAGCCA-3′	690	OL679467	XM_030280649	258-487a.a./ 509a.a.	99% to XP_ 030136509	91% to NP_ 001026739	60% to NP_ 005190

[1]The primers listed were used for cloning the cDNA fragments. Accession numbers are for record in GenBank. The last three columns list the similarity of amino acid sequences, expressed as percentages between cloned fragments and the corresponding nAChRs in zebra finch, chicken, and human, respectively. Human chrnA8 does not exist.

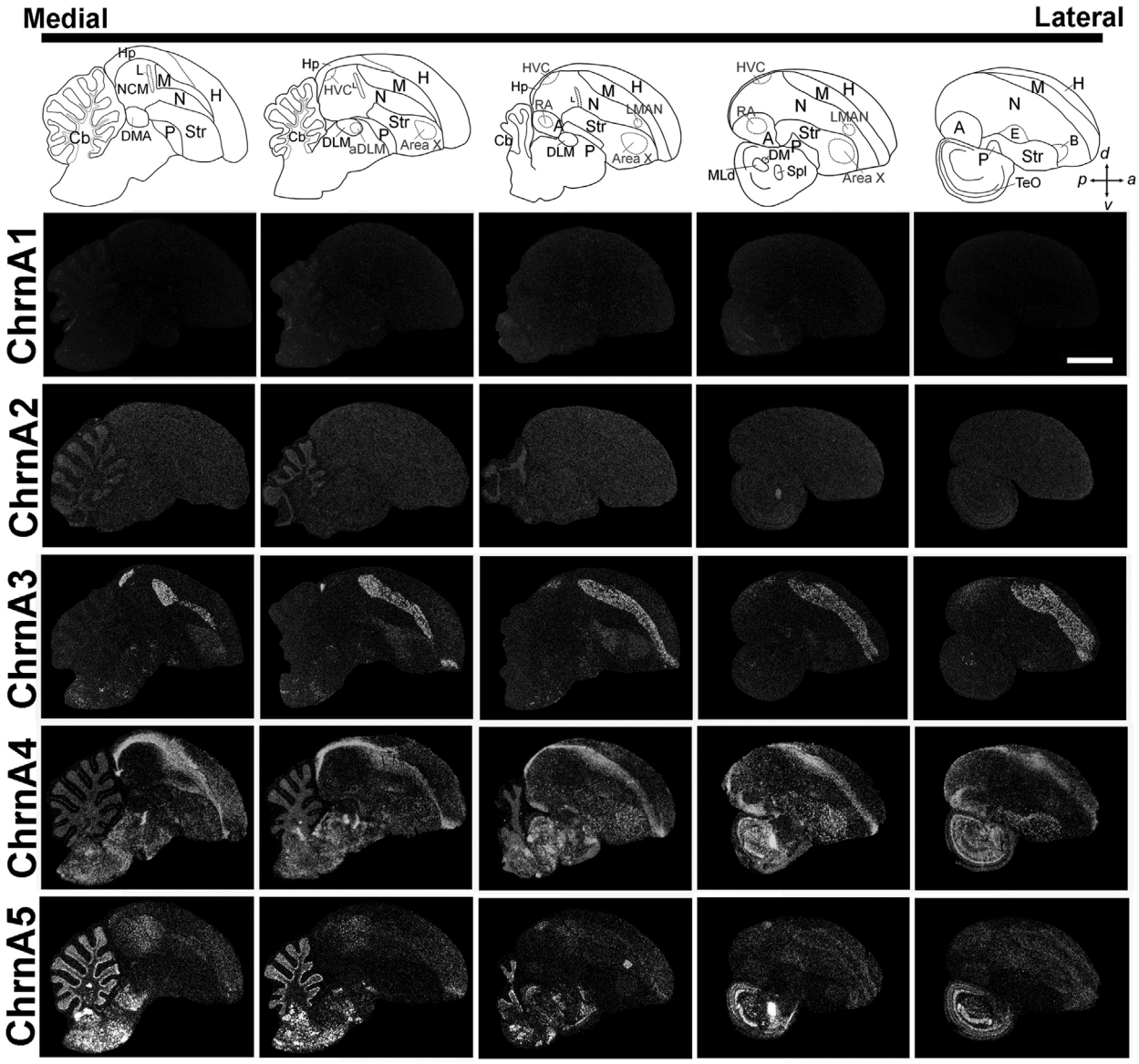

FIGURE 2 Expression of nicotinic acetylcholine receptor A subunits (ChrnA1–5) in the male zebra finch brain. Expression images for each subunit are in a different row, and within rows, images of parasagittal brain sections are organized by medial (left) to lateral (right) progression. Sections are oriented with rostral side to the right, and dorsal side up. Levels of brightness represents levels of the mRNA signal. A camera lucida drawing at the top of each column identifies the brain areas represented in the sections in the column below. Scale bar = 1 mm

sound-attenuating box overnight under silent and dark conditions. The next morning before light onset, the bird under deep anesthesia was perfused with ice-cold cutting buffer (Saunders et al., 2018). Then, the telencephalon was removed and kept in ice-cold cutting buffer until sectioning. Brain sections were cut at 400 μm in the sagittal plane in ice-cold cutting buffer with a microslicer (DTK-1000; Dosaka EM, Kyoto, Japan). HVC and RA tissues were punched out with Miltex Biopsy Punch (1 mm diameter; Ted-pella Inc., Redding, CA, USA), frozen in sample storage buffer with 0.2 U/ml RNase inhibitor (Takara Bio), and 10% DMSO in 1× PBS and stored at −80°C until nuclei isolation. Punched tissues were homogenized in 750 μl of ice-cold Nuclei PURE Lysis Buffer using a glass Dounce tissue grinder (DWK LIFE SCIENCES, Mainz, Germany) (40 times with tight pestle), centrifuged at 500× *g* for 10 min at 4°C, washed with 1 ml of nuclei wash and resuspension buffers. After centrifugation, the supernatant was removed, while the nuclei were suspended in 120 μl of nuclei wash and resuspension buffers with DAPI and filtered with 40 μm cell strainers. Isolated cell nuclei were purified with a cell sorter (SH800; Sony, Tokyo, Japan) using DAPI fluorescence. The 10× Chromium libraries were prepared using Chromium Single Cell Library Kit v3 (PN-1000092, 10× Genomics) according to the manufacturer's protocol. cDNA along with cell barcode identifiers were PCR-amplified, while sequencing libraries were prepared. The constructed library was sequenced on MGI DNBSEQ-G400 (150 bp Paired-end) platform. The Cell Ranger Software Suite (v4.0.0) was used to perform sample de-multiplexing, barcode processing, and single-cell 3′ unique molecular identifier (UMI) counting.

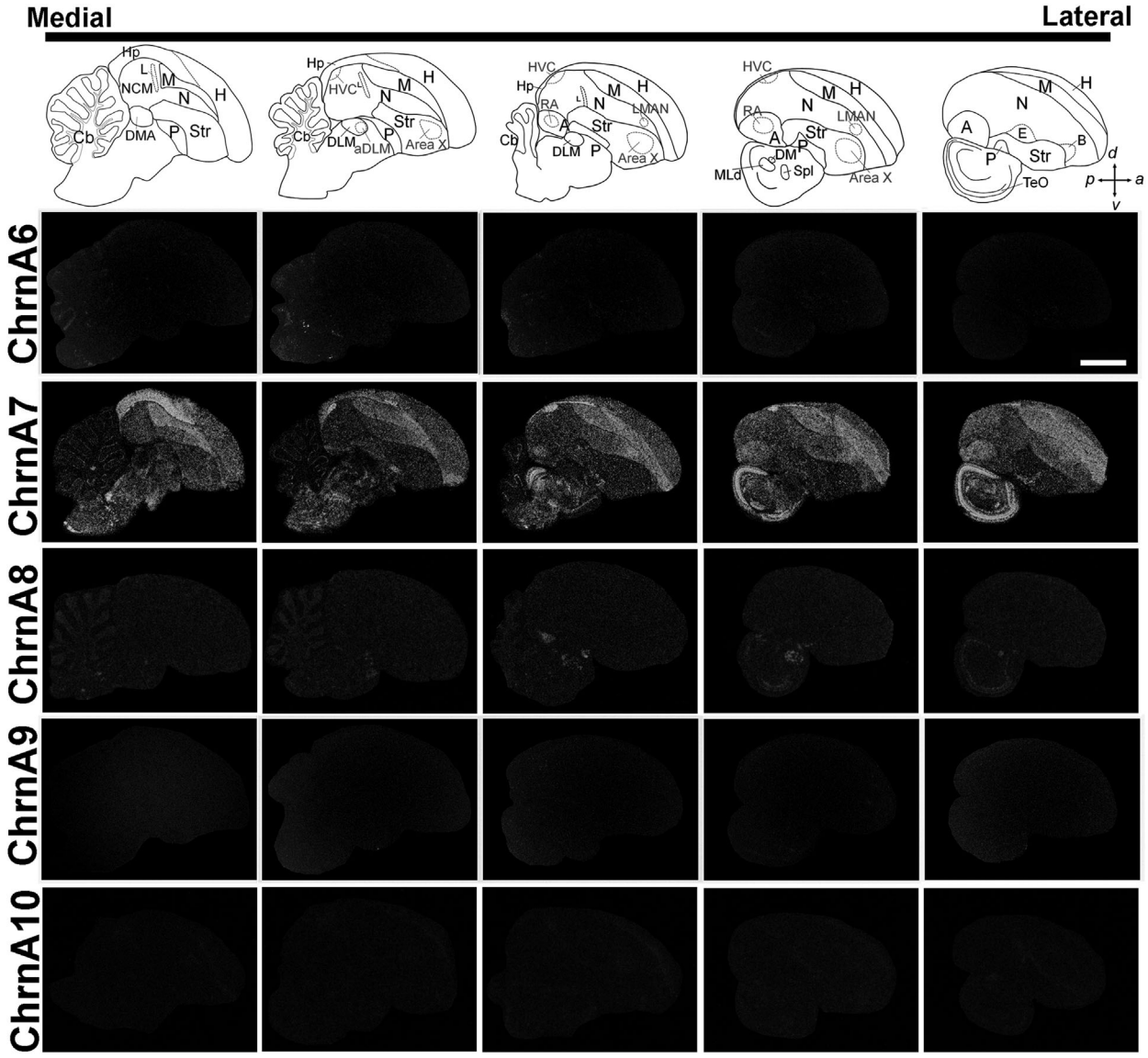

FIGURE 3 Expression of nicotinic acetylcholine receptor A subunits (ChrnA6–10) in the male zebra finch brain. Expression images are arranged as in Figure 2. Scale bar = 1 mm

Splicing-aware aligner STAR was used in FASTQs alignment with a zebra finch reference genome (bTaeGut1_v1.p, GCF_003957565.1 based custom reference genome). Cell barcodes were determined based on the distribution of UMI counts automatically.

2.5 | Cell cluster analysis

The R package Seurat v.3 was used for the following data filtering and analyses (Stuart et al., 2019). Filtering criteria applied to the data, using "CreateSeuratObject," included min.cells = 3, and min.features = 200. After filtering, a total of 6510 and 6977 cells in HVC and RA, respectively, were left for further analysis. The filtered gene-barcode matrix was first normalized using "LogNormalize" methods with default parameters. The top 2000 variable genes were then identified using the "vst" method in Seurat FindVariableFeatures function. Principal component analysis (PCA) was performed using the top 2000 variable genes. Uniform Manifold Approximation and Projection (UMAP) was performed on 27 to 31 principal components for visualizing the cells. Meanwhile, graph-based clustering was performed on the PCA-reduced data for clustering analysis with Seurat v.3. Clusters were determined using "FindNeighbors" (with 27 to 31 principal components) and "FindClusters" (resolution = 1). The expression of established marker genes was used to assign identities for each cluster: SLC17A6 for glutamatergic neurons; GAD1 and GAD2 for GABAergic neurons; SOX4 and SOX11 for neuronal progenitors; SLC15A2, SLC1A2, and ASPA for astrocytes; PDGFRA and NKX2.2 for oligodendrocyte precursor cells (OPCs); PLP1 and ST18 for oligodendrocytes; and CSF1R and IKZF1 for microglia (Saunders et al., 2018; Tasic et al., 2016, 2018; Zhang et al., 2014). Subclusters in glutamatergic neurons

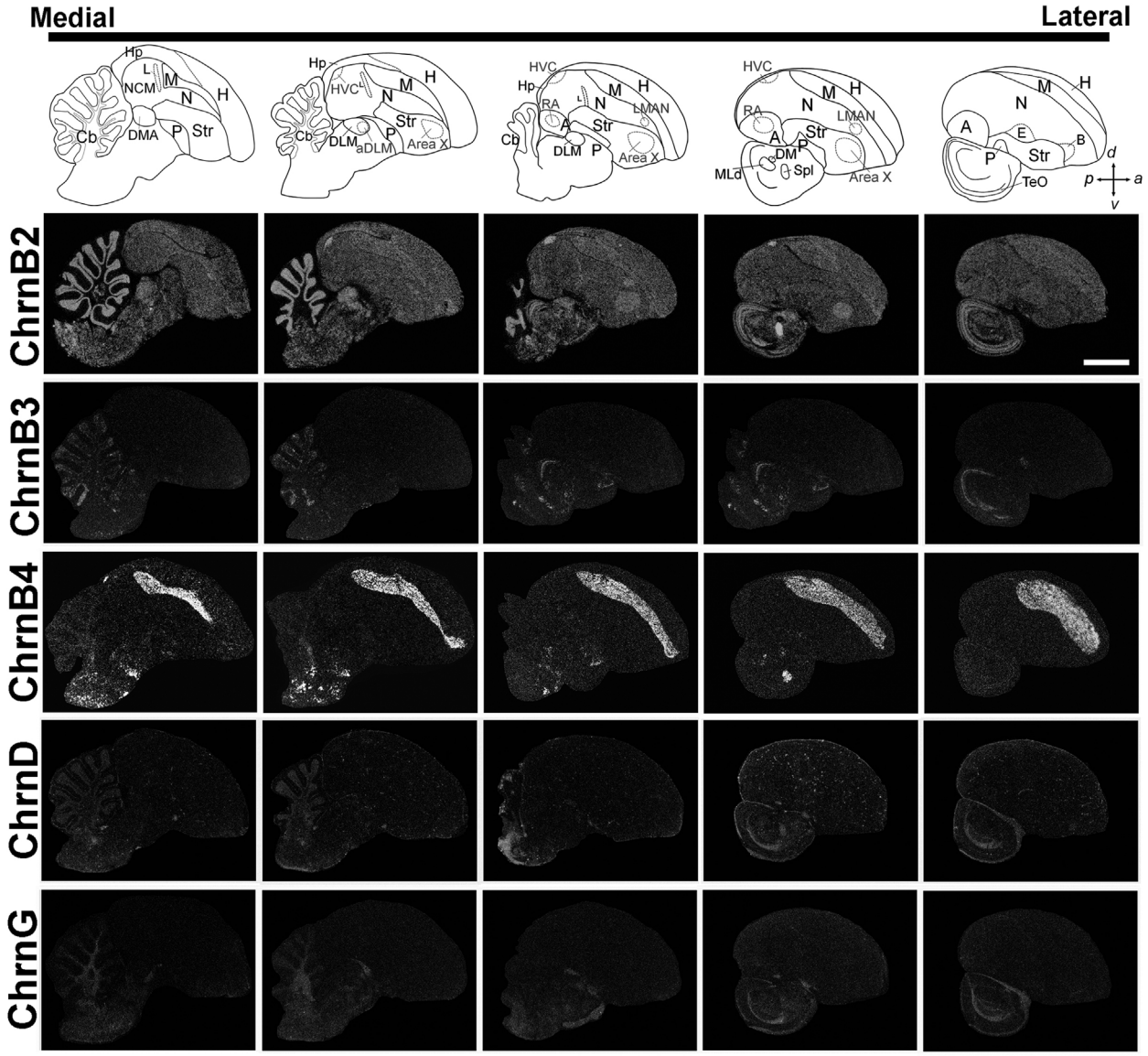

FIGURE 4 Expression of nicotinic acetylcholine receptor B (ChrnB2–4), D, and G subunits in the male zebra finch brain. Expression images are arranged as in Figure 2. Scale bar = 1 mm

in HVC were identified based on a previous report (Colquitt et al., 2021) and in situ hybridization database, ZEBrA (Lovell et al., 2020): GFRA1 and UTS2B were used as marker genes for $HVC_{(RA)}$ neurons projecting to RA (Bell et al., 2019); NTS and SCUBE1 for $HVC_{(X)}$ neurons projecting from HVC to Area X and RA neurons projecting to the nucleus of cranial nerve XII; GRIA4, GRM1, and CACNA2D1 for surrounding caudal nidopallium (cN) neurons; and CACNA1H, MGAT4C, and ADYAP1 for RA surrounding arcopallial neurons. Three unknown clusters with no specific marker gene and several small clusters (less than 60 cells in each) were filtered out. Each neural cell-type was isolated and re-clustered based on the expression of ChrnA3–5, A7, and B2 and two to four other genes specifically expressed in each using PCA implemented in the "RunPCA" function of Seurat. Subtype specific genes included KCNH1 and ROBO2 for $HVC_{(RA)}$ neurons; SRD5A2 and SLIT3 for $HVC_{(X)}$ neurons; SRD5A2 and SLC4A11 for RA projection neurons; GPC6, FOXP2, MAF, and VSTM2A for interneurons; and CELF2, DACH2, LOC115498355, and SDCCAG8 for HVC progenitor neurons. Then, UMAP was performed on all principal components in each cell-type for visualizing cell clusters formation based on CHRN family gene expression patterns.

2.6 | Statistical analyses

Data obtained on the developmental regulation of different AChR subunits were analyzed with statistical software SPSS (IBM Statistics, Armonk, NY, USA). Differences in mRNA expression levels of ChrnA3–5, A7, and B2 in the song nuclei were analyzed after a

test for homogeneity of variance, using one-way analyses of variance (ANOVA) followed, when appropriate, by Scheffe's *F* tests.

3 | RESULTS

3.1 | nAChR subunits expressed in zebra finches

Using cDNAs synthesized from the brain tissues of an adult male zebra finch and oligo-primers specific to protein-coding regions of nAChR, we cloned partial cDNA fragments of all 15 nAChR subunits (ChrnA1−10, B2−4, D, and G) predicted in avian species using RT-PCR (Table 1). The partial cDNAs and the corresponding translated amino acid sequences of the 15 cloned nAChRs were verified by comparing each nAChR subunit transcript predicted for the zebra finch with those previously identified in chicken and human. We confirmed that the match between each cloned partial nAChR subunit and the predicted full-length mRNA of the targeted subunits in the zebra finch was ≥98.6% at nucleotide level and ≥99.3% at protein level (Tables 1 and 2). This result was consistent with the NCBI database prediction of nAChR transcripts from the zebra finch genome and indicated that 15 nAChR subunits were expressed in the zebra finch brain.

To evaluate the confounding cross-hybridization potential of in situ hybridization probes, we calculated the fraction (as a percentage) of sequence identities between each cloned subunit fragment and all nontargeted nAChR subunit protein-coding regions (Table 2). This analysis revealed that while the cloned partial cDNAs had near perfect match (≥98.6% similarity highlighted in red on the diagonal) with their targeted subunit sequences (as described above), the match with any nontargeted cross-nAChR subsequence was ≤76.8% (off-diagonal similarity values). Only 21 (10%) of the 210 off-diagonal values were greater that 50% (entries in various shades of pink). We speculated that this level of mismatch was sufficient to avoid confounds from cross-hybridization with nontargeted nAChR subunits.

The cloned partial fragments of ChrnA1−10, B2−4, D, and G were used in in situ hybridization experiments to reveal the distribution of nAChR subunit expression in the brain tissues of adult male zebra finches. Eleven (ChrnA2−5, A7, A8, B2−4, D, and G) of the 15 cloned subunits were expressed in unique patterns in at least one of the following brain regions: pallium, thalamus, midbrain, and cerebellum (Figures 2–4). In contrast, the four remaining receptor subunits, ChrnA1, A6, A9, and A10, exhibited few or no detectable mRNA signals throughout the whole brain. Therefore, no further investigations into mRNA expression were conducted for these four subunits.

3.2 | Expression of nAChR subunits in telencephalic subregions

The pattern of mRNA expression and amount of each nAChR subunit available were evaluated in the following five major pallial telencephalic brain subdivisions: hyperpallium, mesopallium, nidopallium, arcopallium, and hippocampus. ChrnA4 and A7 were highly expressed in the mesopallium, arcopallium, and hippocampus compared with the other pallial subdivisions (Figures 2, 3, and 5). In contrast, ChrnA2, A5, and B2 showed consistent but relatively low-level expression within all telencephalic subdivisions. As distinct exceptions, ChrnA3 and B4 showed similar expression patterns, strictly restricted to the mesopallium. Taken together, the mRNA for ChrnA3, A4, A7, and B4 exhibited a higher level of expression in the mesopallium than in the other pallial subdivisions (Figure 5).

Consistent with the pattern of nAChR subunit expression in the nidopallium, mRNAs of ChrnA2, A7, and B2 were uniformly throughout the caudomedial nidopallium (NCM), which is known as the avian secondary auditory area (Figure 6). Conversely, ChrnA5 expression was more restricted to the rostral portion of NCM, where its expression was higher than in the anterior nidopallium. ChrnA3, A4, and B4 were expressed at very low or undetectable levels in NCM as in most of the other nidopallial regions.

Subunits ChrnA4 and ChrnA7 showed differential expression in the subdomains (Mello et al., 2019) of the arcopallium (Figure 7a). ChrnA4 was intensely expressed in most arcopallial subdomains except in the dorsal part of AI (AId), where it was almost fully suppressed. ChrnA7 distinctly showed higher expression in the caudal areas, including AD and the ventral part of AP, than in all other subdomains. ChrnA2, A5, and B2 were expressed with nearly uniform intensities at low-to-moderate levels throughout the subdomains of the arcopallium. ChrnA3 and B4 expressions were undetectable. Quite uniquely, ChrnA8 mRNA expression was well-defined and confined in the intermediate part of the medial ventral arcopallium (AMVi), so-called nucleus taenia (TnA) (Figure 7b).

The primary sensory input regions located within the nidopallium, including field L (auditory), entopallium (visual), and nucleus basorostralis (somatosensory/trigeminal), are anatomically defined in Nissl-stained tissue by a higher cell density relative to the surrounding nidopallium. While ChnrA2 mRNA was lightly expressed with near uniform intensity in each surrounding region of the nidopallium, expression of all other nAChR subunits was apparently absent in the primary sensory input regions (Figures 2–4). Similarly, ChrnA3, A5, and B4 expressions were suppressed in the subpallial striatum and globus pallidus. In contrast, ChrnA4 was uniquely expressed in the striatal region, with small dots, suggesting its selective expression in a specific cell type (Figure 2). The cells labeled for ChrnA4 expression, shown as intense isolated small dots, were clearly identified as a sparse cell population in the striatum by the zebra finch expression brain (ZEBrA) atlas based on digoxigenin-based labeling in situ hybridization method. Similarly, ChrnB3 mRNA expression was observed specifically in the lateral pallium (Figure 4). In contrast, ChrnA2, A7, and B2 expressions in the striatum and pallidum were similar to those in pallial regions.

In the hippocampus, we observed a unique form of nAChR subunit specialization that was further portrayed according to the delineation of the hippocampus into dorsal and ventral subdivisions (Figure 8) with ChrnA3 expression occurring dorsally and ChrnA4 and A7 ventrally, suggesting a potential distinction of ACh function between the proximal and distal parts. Furthermore, ChrnA4 and A7 were even more expressed in the mesopallium, exhibiting seamless expression

TABLE 2 Sequence similarities between complementary DNAs (cDNAs) and the protein-coding regions of 15 nicotinic acetylcholine receptors (nAChR) subunits in the zebra finch[1]

Predicted zebra finch nAChR subunits		Cloned partial cDNAs to make in situ hybridization probes														
GenBank accession No.	nAChR subunits	ChrnA1	ChrnA2	ChrnA3	ChrnA4	ChrnA5	ChrnA6	ChrnA7	ChrnA8	ChrnA9	ChrnA10	ChrnB2	ChrnB3	ChrnB4	ChrnD	ChrnG
XM_002199046	ChrnA1	99.7	30.3	16.1	58.0	20.3	23.3	0.0	0.0	0.0	0.0	31.6	12.0	30.2	0.0	0.0
XM_041715494	ChrnA2	61.4	100.0	38.4	76.8	45.0	0.0	1.7	0.0	0.0	62.0	68.9	8.8	7.0	26.7	0.0
XM_012569079	ChrnA3	30.0	25.3	99.9	66.8	51.6	54.0	0.0	0.0	5.1	0.0	34.2	0.0	11.1	8.9	0.0
XM_012570240	ChrnA4	60.0	47.9	42.2	99.1	48.4	42.5	4.7	2.6	27.0	0.0	66.9	9.7	42.3	29.7	0.0
XM_030281197	ChrnA5	13.2	19.9	33.1	36.4	100.0	36.7	12.5	0.0	30.3	0.0	14.0	0.0	18.5	3.3	0.0
XM_002188838	ChrnA6	37.2	0.0	53.4	56.0	61.6	99.8	0.0	4.0	27.1	0.0	12.0	0.0	33.4	4.8	0.0
XM_030281037	ChrnA7	0.0	2.5	0.0	1.9	19.7	0.0	99.7	30.2	0.0	0.0	0.0	4.3	0.0	0.0	0.0
XM_002187662	ChrnA8 (7-like)	0.0	0.0	1.0	5.3	22.6	1.0	53.3	99.1	0.0	0.0	4.5	0.0	11.9	0.0	0.0
XM_030270964	ChrnA9	9.2	0.0	0.0	15.5	16.9	8.2	0.0	6.9	100.0	67.9	1.9	0.0	12.1	0.0	0.0
XM_030284731	ChrnA10	0.0	24.5	0.0	46.5	0.0	0.0	0.0	0.0	64.5	99.0	39.9	0.0	0.0	16.6	0.0
XM_030291667	ChrnB2	30.5	44.2	25.8	58.4	19.6	18.3	0.0	0.0	0.0	37.4	99.3	0.0	67.0	21.1	19.7
XM_002189012	ChrnB3	34.9	3.7	35.6	57.1	70.9	0.0	1.0	0.0	0.0	0.0	0.0	99.7	0.0	4.5	0.0
XM_030281195	ChrnB4	24.8	0.0	10.4	49.7	22.2	29.6	0.0	0.0	0.0	0.0	72.9	0.0	100.0	14.0	0.0
XM_030280650	ChrnD	0.0	29.3	9.6	12.9	4.1	5.6	0.0	0.0	0.0	43.9	46.3	0.0	21.9	99.4	22.7
XM_030280649	ChrnG	4.1	0.0	2.5	0.0	0.0	0.0	0.0	0.0	0.0	0.0	63.1	0.0	4.2	40.2	98.6

[1]Matching base-pair sequences as a fraction of the length of cDNAs are shown as percentages. High similarity values (≥98.5%) on the diagonal (cells highlighted in red) shown on-target identity. Perfect dissimilarity with off-target subunits is represented by a zero in an off-diagonal entry. Because the full-length transcript is expected to be expressed in cells, nonzero off-diagonal similarity values indicate the potential for in situ cross-hybridization of each subunit cDNA fragment to 14 off-target subunits. The low off-diagonal similarity values (≤76.8%) indicate that the potential for such confounds was low.

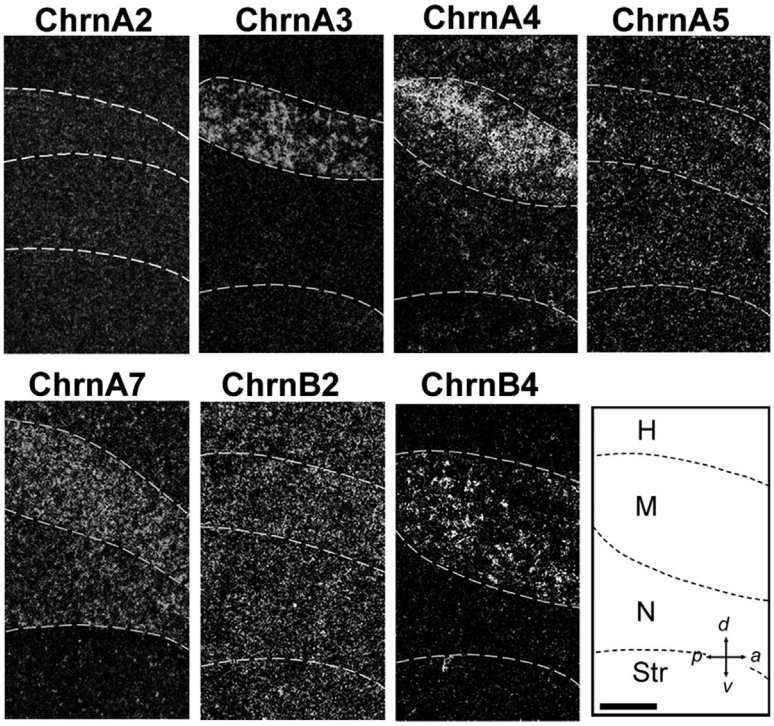

FIGURE 5 Expression of nicotinic acetylcholine receptor (nAChR) subunits in subdivisions of the anterior pallial regions. In situ hybridization images for ChrnA2–5, A7, B2, and B4. Camera lucida drawing (bottom right panel) shows boundaries of the major subdivisions (H, hyperpallium; M, mesopallium; N, nidopallium; Str, Striatum) of these brain regions in exact correspondence to the orange dotted lines in the ChrnB4 image, and approximately for all others. Scale bar = 3 mm for all images

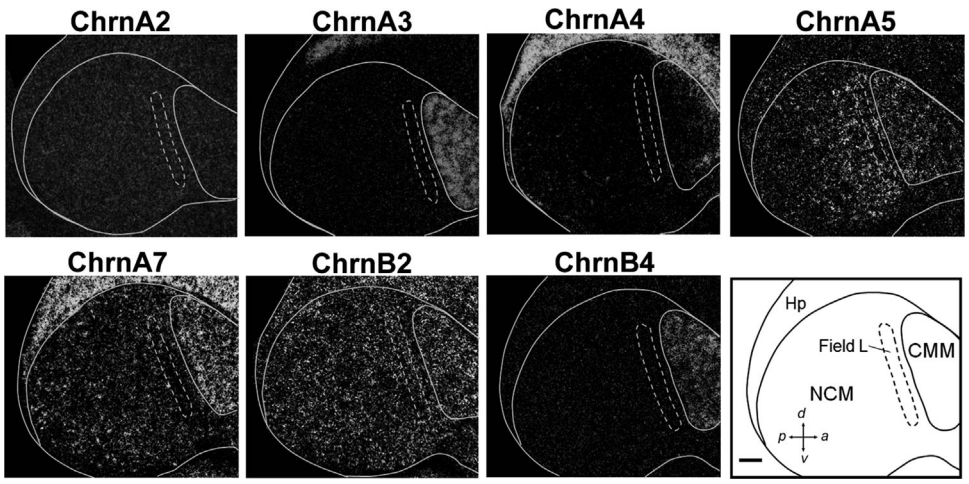

FIGURE 6 Expression of nicotinic acetylcholine receptor (nAChR) subunits in subdivisions of the posterior medial pallial regions. In situ hybridization images for ChrnA2–5, A7, B2, and B4. Bottom right: camera lucida drawing showing major subdivisions (Hp, hippocampus; NCM, caudomedial nidopallium; CMM, caudomedial mesopallium of the brain) of these brain regions. Scale bar = 3 mm

from the mesopallium to the ventral hippocampus. Notably, the expression of ChrnA3 was also confined to the medial caudal part of the hippocampus (Figure 2). In contrast to these selective expressions of ChrnA3, A4, and A7 subunits, ChrnA2 and B2 were expressed equally in the dorsal and ventral hippocampus. However, ChrnA5 and B4 expression levels were nearly undetectable in the hippocampus.

3.3 | Expression of nAChR subunits in the midbrain and cerebellum

Further investigation revealed more specializations for ChrnA2–5, A7, A8, and B2–B4 in the nuclei/parts of the midbrain (Figure 9). Specifically, the nucleus pretectalis (Pt) and spiriform lateralis (Spl) were strongly labeled by ChrnA2, A4, A5, A7, and B2. While ChrnA4 and A5 were more intensely expressed both in Pt and Spl than in other midbrain nuclei, ChrnA7 was selectively expressed only in Pt. Conversely, ChrnA2 and B2 mRNA expressions were higher in Spl than in Pt. However, the expression of these subunits was almost completely suppressed below signal detection in the nucleus rotundus (Rt). There were exceptions, suggesting a selective cell type expression in Rt: ChrnA2 and B2 were observed with low-to-moderate expression, and ChrnA8, with sporadic expression. ChrnA2, A5, and B2 showed low-level expression in the dorsomedial nucleus of the midbrain (DM), namely, the midbrain vocal center, and the nucleus mesencephalicus

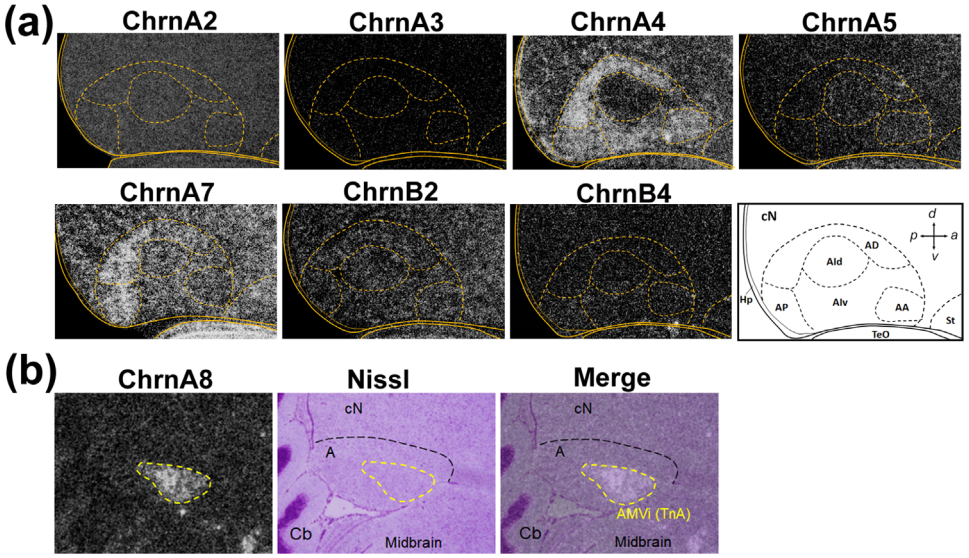

FIGURE 7 Expression of nicotinic acetylcholine receptor (nAChR) subunits in subdivisions of the arcopallium. (a) In situ hybridization images for ChrnA2–5, A7, B2, and B4 in the lateral arcopallial regions. Camera lucida drawing (lower right) shows major subdivisions of this region of the brain. Orange dotted lines represent the borders of brain subdivisions: the anterior, posterior, dorsal, and intermediate arcopallium denoted by AA, AP, AD, and AI, respectively. AId and AIv: dorsal and ventral subdivisions of AI, respectively. cN: caudal nidopallium. (b) Specific expression of ChrnA8 in the intermediate part of the medial ventral arcopallium (AMVi), also called nucleus taenia (TnA)

FIGURE 8 Expression of nicotinic acetylcholine receptor (nAChR) subunits in subdivisions of the hippocampus. In situ hybridization images for ChrnA2–5, A7, B2, and B4. Camera lucida drawing (lower right panel) shows the dorsal (Hpd) and ventral (Hpv) subdivisions of the hippocampus. cN: caudal nidopallium. Scale bar = 3 mm

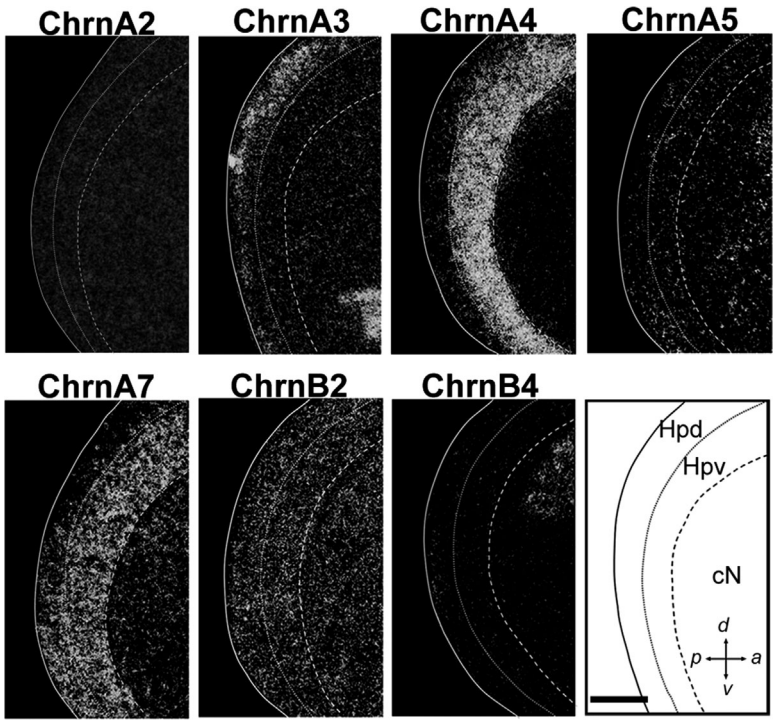

lateralis pars dorsalis (MLd), which forms the avian homologue of the central nucleus of the mammalian inferior colliculus (Boord, 1968; Woolley & Portfors, 2013). In addition, ChrnA7 mRNA was selectively expressed in the ventral part of MLd (near the 3rd ventricle). However, most nAChR subunits were undetected in these regions. The nuclei subpretectalis (SP) and isthmi pars parvocellularis (IPc) play crucial roles in the regulation of visual figure-ground discrimination (Schryver & Mysore, 2019; Scully et al., 2014). Here, ChrnB4 showed clear and specific expression in SP, while in contrast, IPc was labeled with high levels of ChrnA4, A5, and B3 expression (but ChrnA4 expression was suppressed in the lateral part of IPc; Figure 2). Overall, these results indicated that nAChR subunits are expressed

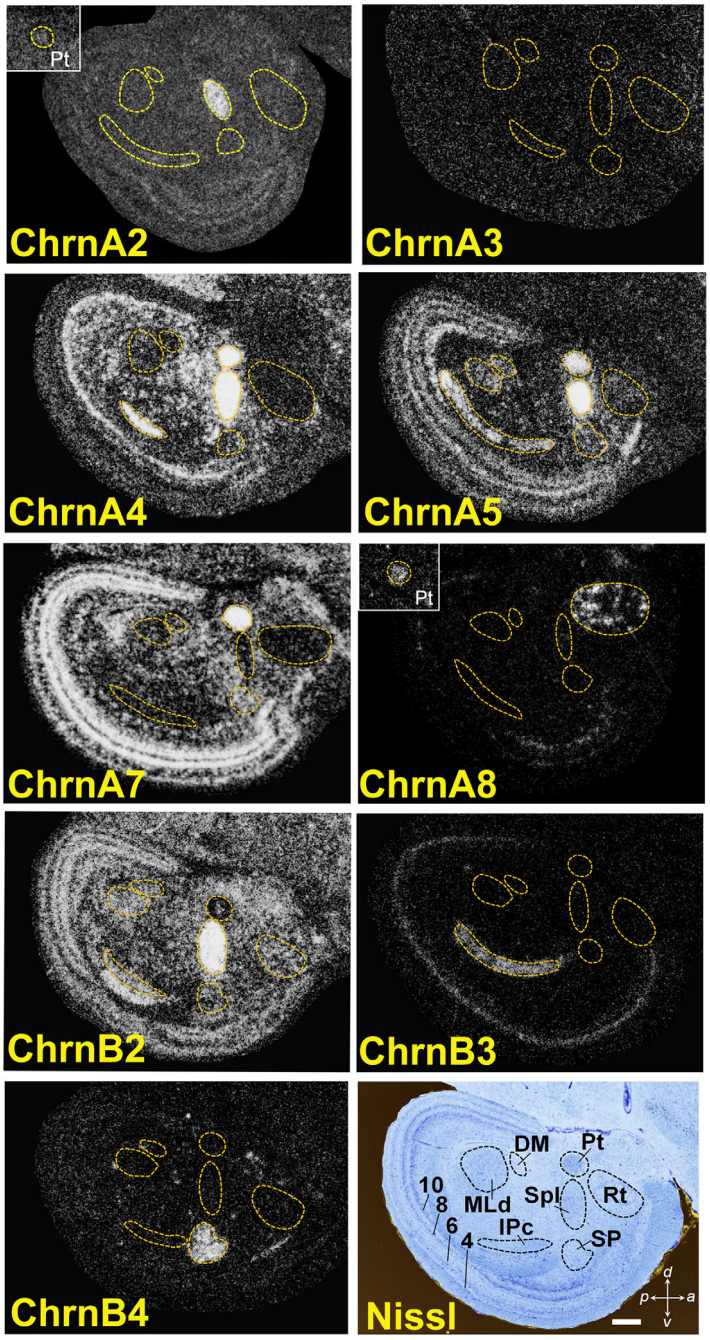

FIGURE 9 Expression of nicotinic acetylcholine receptor (nAChR) subunits in the midbrain. In situ hybridization images for ChrnA2–5, A7, A8, and B2–4. Orange dotted lines show the borders of nuclei/parts in the midbrain. Right bottom: Nissl-stained brain image showing midbrain nuclei: Pt, nucleus pretectalis; Spl, nucleus spiriform lateralis; Rt, nucleus rotundus; DM, nucleus dorsomedialis of the midbrain; MLd, nucleus mesencephalicus lateralis, pars dorsalis; SP, nucleus; IPc, nucleus isthmi pars parvocellularis. Arabic numerals represent clearly identified layers of the tectum opticum. Scale bar = 3 mm

differently in various combinations in the subnuclei/parts of the midbrain.

The layers of tectum opticum (TeO) also revealed distinct patterns of nAChR subunit distribution. According to Cajal's definition (Ramon y Cajal, 1911), there are about 15 histologically identifiable layers in the avian TeO (Wylie et al., 2009). In this study, five layers (layers 4, 6, 8, 10, and 13) were clearly differentiated according to the labeling patterns/intensities of ChrnA2, A4, A5, A7, A8, B2, and B3 mRNAs (Figure 9). Unlike ChrnA3 and B4, whose expression is clear in the mesopallium, these subunits were completely downregulated in all identified layers and subnuclei of TeO. ChrnA4, A7, A8, and B3 were more highly expressed in the deeper layers (layers 8–13) than in the more peripheral layers (layers 4–6), although their downregulation was not as great as that of ChrnA3 and B4. However, ChrnA2, A5, and B2 showed moderate-to-high levels of expression in all of the identified tectal layers.

We further examined the expression patterns of ChrnA2–5, A7, B2–4, D, and G in four anatomical layers of the cerebellum (the molecular, Purkinje cell, granular, and white matter layers). However, even though ChrnA2, D, and G were expressed in the granular layer, their mRNA signals were very weak (Figure 10), and those for ChrnA3 and B4 mRNA were almost undetectable. Moreover, whereas ChrnA4 and B2 were clearly expressed in the granular layer, ChrnA7 was selectively expressed in Purkinje cell layer. The expression of ChrnA5 was intense

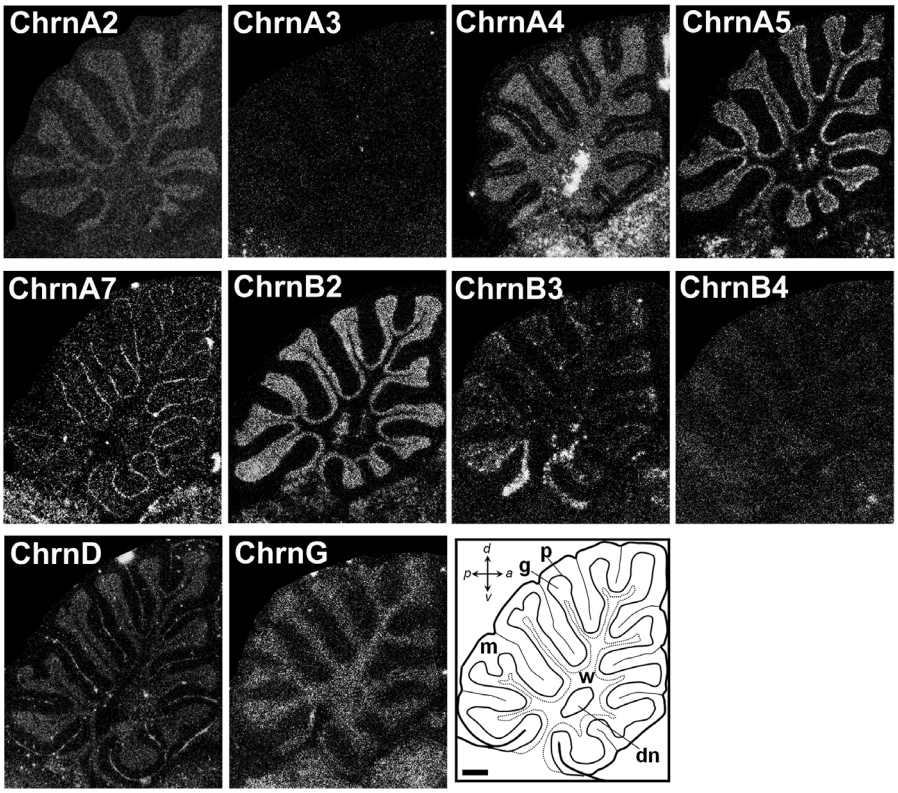

FIGURE 10 Expression of nicotinic acetylcholine receptor (nAChR) subunits in the cerebellum. In situ hybridization images for ChrnA2–5, A7, B2–4, D, and G. Camera lucida showing sublayers of the cerebellum; p = Purkinje layer, m = molecular layer, g = granular layer, w = white matter, dn = deep nucleus. Scale bar = 3 mm

in both the granular and Purkinje cell layers, while ChrnB3 showed selective stronger expression at the top and bottom parts of the granular layer than in other parts of the cerebellum.

Overall, the expressions of four of the 15 cloned AChR subunits (ChrnA1, A6, A9, and A10) were very low or below detectable levels throughout the entire brain. However, expression of 11 subunits (ChrnA2–5, A7, A8, B2–4, D, and G) showed unique combinations of spatial patterns and intensities in at least one subregion of the pallium, thalamus, midbrain, and cerebellum (Figure 11).

3.4 | Differential expression of nAChR subunits in song nuclei

Of the 15 nAChR subunits cloned from the male zebra finch, six (ChrnA2–5, A7, and B2) were expressed in the following song nuclei at the adult stage: HVC and RA in the VMP; and LMAN, Area X, and aDLM in the AFP (Figures 2–4). Expression of ChrnA2 in these song nuclei was not differentially regulated against the surrounding regions, but the five other subunits showed differential expression in one or more song nuclei compared with their surrounding regions.

Four of these differentially regulated subunits, ChrnA3, A5, A7, and B2, were expressed at higher levels in the premotor song nucleus HVC than the surrounding caudal nidopallium (Figure 12). In particular, ChrnA3 mRNA was expressed in limited HVC cells, whereas the other subunits showed a uniform expression pattern throughout HVC. In addition, the expression of ChrnA5 and B2 was clearly higher in LMAN relative to the surrounding rostral nidopallium. Although ChrnA7 was certainly expressed in LMAN, its expression was not specialized in comparison with that in the surrounding area (Figure 12a). In addition, ChrnA5, B2, and other subunits were not differentially expressed in the shell subregion of LMAN (Bottjer & Altenau, 2010) relative to the surrounding nidopallium.

Conversely, the expression of ChrnA4 was lower in RA than in the surrounding arcopallium. Although none of the nAChR subunits exhibited higher levels of expression in RA and Area X relative to the surrounding arcopallium and striatum, respectively, low-to-moderate expression was observed in RA (for ChrnA7 and B2) and Area X (for ChrnA4 and B2) compared with the respective surrounding brain areas. In aDLM, only ChrnA5 showed a higher differential expression level than the surrounding DLM.

Although differences in the expression of glutamate receptors are observed between the lateral and the medial parts of the AFP song nuclei (Wada et al., 2004), two nAChR subunits that were expressed with higher levels in LMAN (ChrnA5 and B2) and in aDLM (ChrnA5) relative to their respective surrounding area did not show differential expressions in the medial MAN and dorsomedial nucleus of the posterior thalamus.

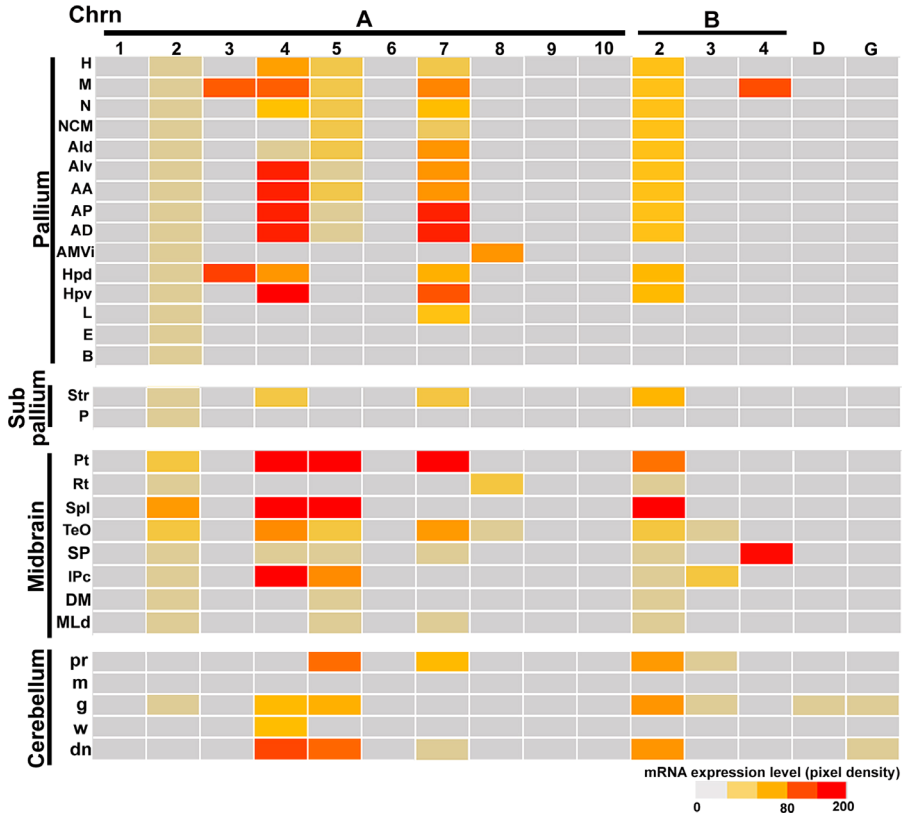

FIGURE 11 Heatmap summarizing the expression of nicotinic acetylcholine receptor (nAChR) subunits in subregions of the zebra finch brain. Levels of expression were measured by image pixel intensity and represented in the heatmap by five-grading colors (color bar)

3.5 | Developmental regulation of nAChR subunits during the critical period of song learning

To examine a potential developmental change in the expression of nAChR subunits in the song nuclei (HVC, RA, LMAN, Area X, and aDLM) through the critical period of song learning, we quantified the mRNA expression levels of ChrnA3−5, A7, and B2. Male zebra finches at the subsong (35−45 phd), plastic song (50−65 phd), and crystallized song (120−140 phd) stages were used. Although nAChR subunits were expressed to varying degrees among the song nuclei, only ChrnA5 showed significantly different regulation in the song nucleus LMAN, with its expression level increased from subsong to crystallized stages (one-way ANOVA followed by Scheffe's F tests, $^{*}p = .031$) (Figure 12b). However, even though the shell subregion of LMAN is implicated in song learning in juvenile zebra finches (Bottjer & Altenau, 2010), the expressions of ChrnA5 and other subunits were not differentially regulated through the critical period of song learning. In addition, although the expression levels of ChrnA5 in Area X increased gradually from the subsong to crystallized song stage, the difference was not statistically significant due to individual variability in the mRNA expression level at the plastic and crystallized song stages. These results indicate that the expression of most nAChR subunits was consistently regulated in the song nuclei throughout song development.

3.6 | Cell type-specific expression of nAChR subunit in the song nuclei

To elucidate the expression of nAChR subunits in different cell types of the vocal motor nuclei HVC and RA, in which the ACh content and related enzyme activity change markedly during the critical period for song learning (Sakaguchi & Saito, 1989), we performed scRNA-seq with the two song nuclei from an adult male zebra finch. Based on the data obtained, we analyzed the expression of ChrnA1−10, B2−4, and D, and G mRNAs in different cell types, including glutamatergic excitatory neurons (including $HVC_{(X)}$, $HVC_{(RA)}$, and RA projecting neurons), GABAergic neurons, progenitor neurons, astrocytes, microglia, oligodendrocytes, OPC, and surrounding excitatory neurons in the nidopallium and arcopallium (Figures 13–16). Consistent with earlier in situ hybridization results, the scRNA-seq data revealed that ChrnA1, A9, B3, B4, and D were expressed only in a few cells in both HVC and RA, while ChrnA6 mRNA was not detected. An exceptional discrepancy in mRNA detection was observed between in situ hybridization and snRNA-seq for ChrnA2 and ChrnA10. Although in situ hybridization revealed adequate expression of ChrnA2 mRNA throughout the entire brain, including HVC and RA, scRNA-seq showed no ChnrA2 (+) cells in both HVC and RA. Conversely, ChrnA10 expression level was almost undetectable by in situ hybridization, whereas snRNA-seq showed several excitatory and inhibitory neurons and astrocytes labeled as

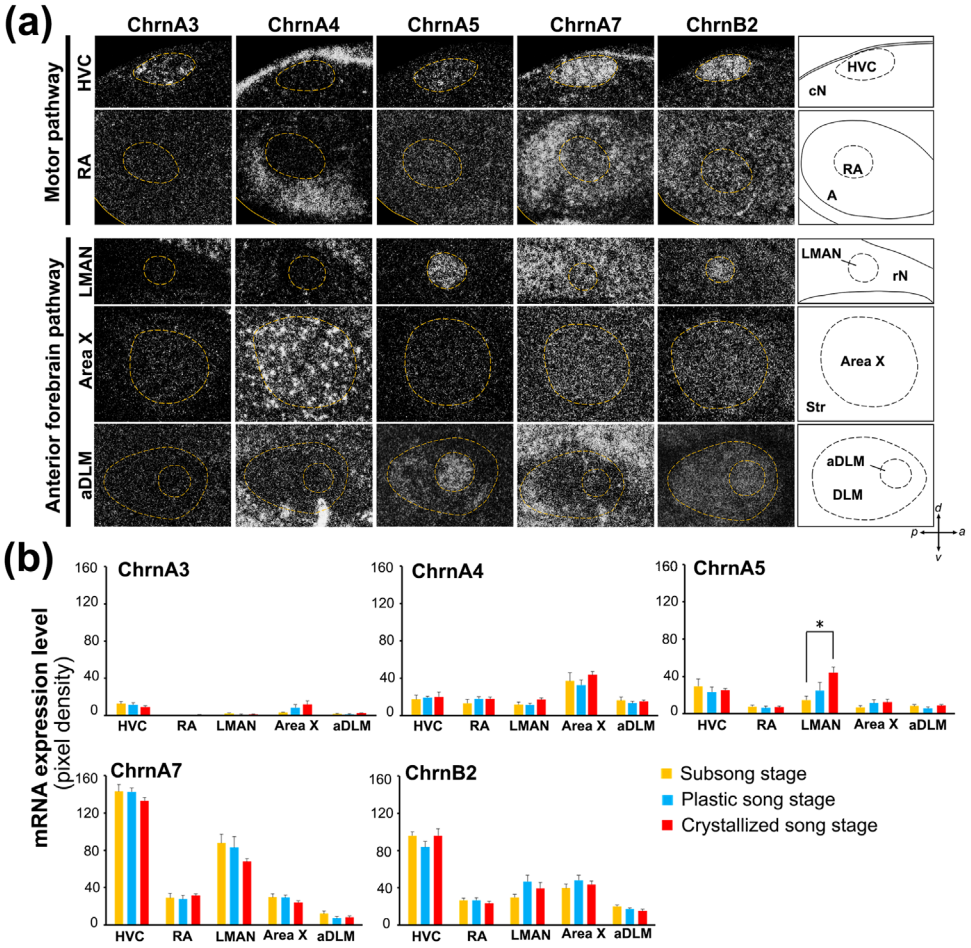

FIGURE 12 Expression of nicotinic acetylcholine receptor (nAChR) subunits in the song nuclei of adult male zebra finches. (a) ChrnA3–5, A7, and B2 expression in song nuclei, HVC, RA, LMAN, Area X, and aDLM. Brains are sagittal, white color represents mRNA signal. Right panels: Camera lucida drawings depicting each song nucleus. Dotted dark lines show the borders of the song nuclei. (b) nAChR subunit expression in the song nuclei during song development. ChrnA3–5, A7, and B2 expression in HVC, RA, LMAN, Area X, and aDLM during the subsong (35–45 phd, orange), plastic song (50–65 phd, blue), and crystallized song (120–140 phd, red) stages of song development. Bars: mean ± *SEM*. $n = 6$ birds/each stage. One-way analysis of variance (ANOVA) $^{*}p < .05$

expressing ChnrA10. Despite our best effort to carefully evaluate the specificity of the in situ hybridization probe and gene annotation information used for scRNA-seq analysis, the inconsistent detection of ChrnA2 and A10 mRNAs remains unclear.

In contrast to those subunits with low or undetectable expression levels, ChrnA3–5, A7, A8, B2, and G were expressed in at least one cell type in these song nuclei at varying levels and in different numbers of cells (Figures 14 and 16). In particular, ChrnA7 and B2 were expressed in most cell types of HVC and RA. As for the results from in situ hybridization (Figure 12a), ChrnA3 expression was biased in selective cell populations of $HVC_{(RA)}$ and $HVC_{(X)}$ projecting neurons and in a few RA projecting neurons. Although very few glutamatergic projecting neurons in HVC and RA expressed ChrnA4, progenitor neurons for HVC and OPC in both HVC and RA showed clear and intense expression of this subunit. ChrnA8 was selectively expressed in a subtype of astrocytes in HVC but not in RA, while ChrnG was selectively expressed in a few oligodendrocyte populations in these song nuclei. In addition, in situ hybridization signals for ChnrA8 and G mRNA were very subtle. Taken together, the scRNA-seq analysis revealed both nonspecific expressions of ChrnA7 and B2 among various cell types and much selective expression of ChrnA3–5, A8, and G in limited cell types, suggesting that there are potentially unique nAChR subunit combinations at the single-cell level in the vocal motor song nuclei HVC and RA.

Since nAChR subunits form heteromeric or homomeric pentamers, which possess different physiological and pharmacological properties (Albuquerque et al., 2009; Gotti et al., 2009; M. Zoli et al., 2015), we further investigated the potential combinations of nAChR subunits coexpressed in neuronal cell types of HVC and RA by focusing on ChrnA3–5, A7, and B2 (Figure 17), which were detected in the song nuclei by in situ hybridization. The results revealed that limited populations of each neuron type expressed only specific nAChR subunits. For instance, although ChrnA3, A5, A7, and B2 were expressed in $HVC_{(RA)}$ neurons, 55% of $HVC_{(RA)}$ neurons showed no expression of nAChR subunits. In addition, most of the remaining $HVC_{(RA)}$ neurons expressed only a single type of nAChR subunit. The selective expression of nAChR subunits was similarly observed in other neuron types in HVC and

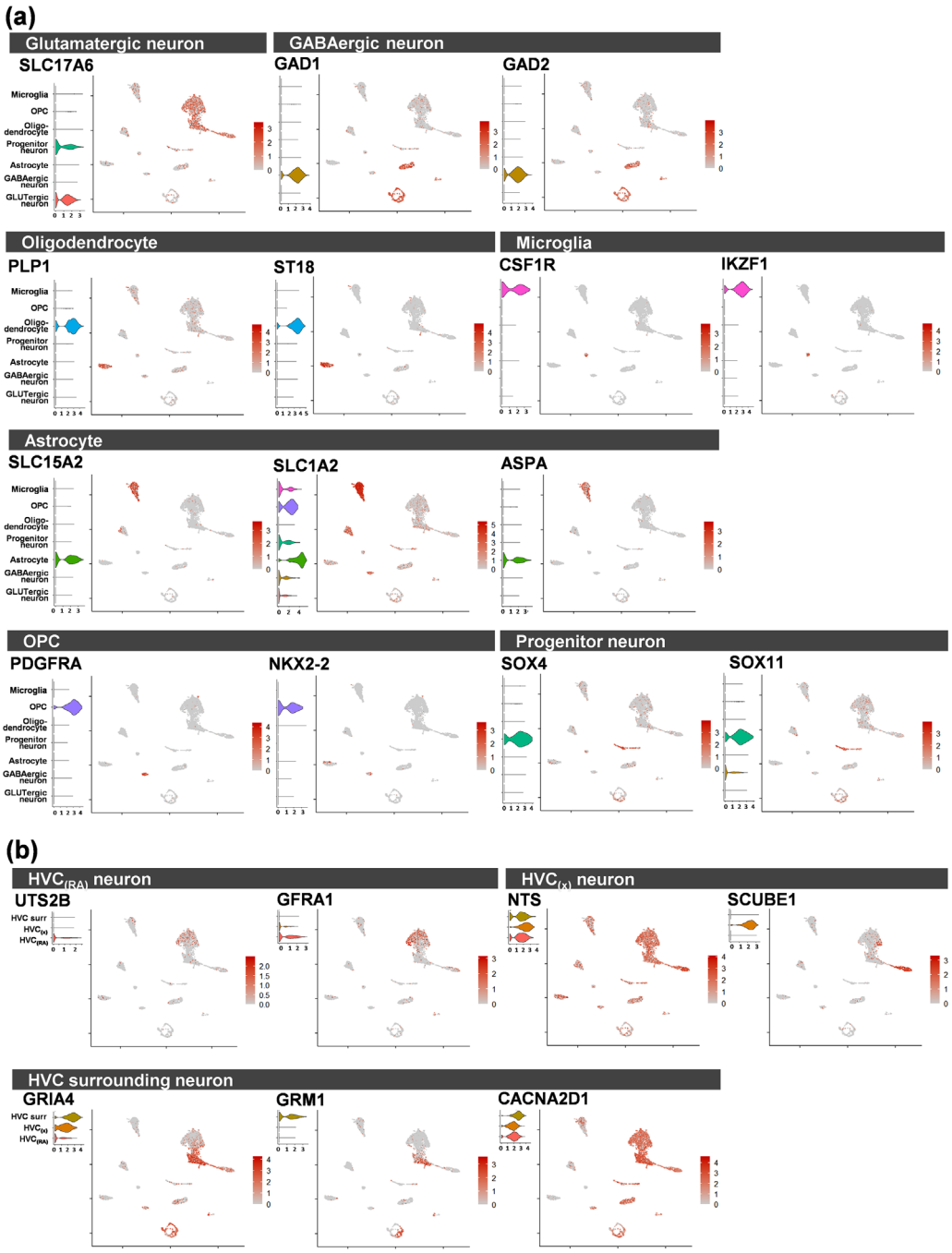

FIGURE 13 Expression of marker genes at each cell-type in HVC. Violin (left side panel) and Uniform Manifold Approximation and Projection (UMAP; right side panel) plots of cell clusters expressing major cell type marker genes (a) and subtype marker of glutamatergic neuron (b)

RA: $HVC_{(X)}$ neurons, interneurons, and progenitor neurons in HVC and projecting neurons and interneurons in RA. ChrnA7 subunits are known to form homomeric nAChRs, while other α subunits (ChrnA2–6) combine with β subunits to form heteromeric receptors (Gotti et al., 2009; M. Zoli et al., 2015). Indeed, we found that ChrnA7 was expressed in some populations of all neuron types in HVC and RA (29% of $HVC_{(RA)}$, 62% of $HVC_{(X)}$, 12% of HVC interneurons, 5% of HVC progenitor neurons, 32% of RA projecting neurons, and 10% of RA interneurons), suggesting the potential existence of ChrnA7-homomeric receptors in these neural cell types. Because the expressions of ChrnB3 and B4 were detected only in a few cells in HVC and RA (Figures 4, 14, and 16), ChrnB2 must be the main β subunit of heteromeric nAChRs in the song nuclei. Our snRNA-seq data revealed that 10%–22% of the neural cell types in HVC and RA expressed ChrnB2 (Figure 17a,b). It is necessary to recognize potential technical limitations of scRNA-seq in detecting the transcribed mRNAs at low levels; even though we counted at least 1 UMI of the scRNA-seq reads as a positive expression of each nAChR subunit, cells coexpressing ChnB2 and other α subunits comprised only a 2%–20% fraction of each neural cell type in HVC and RA. When we focused especially on

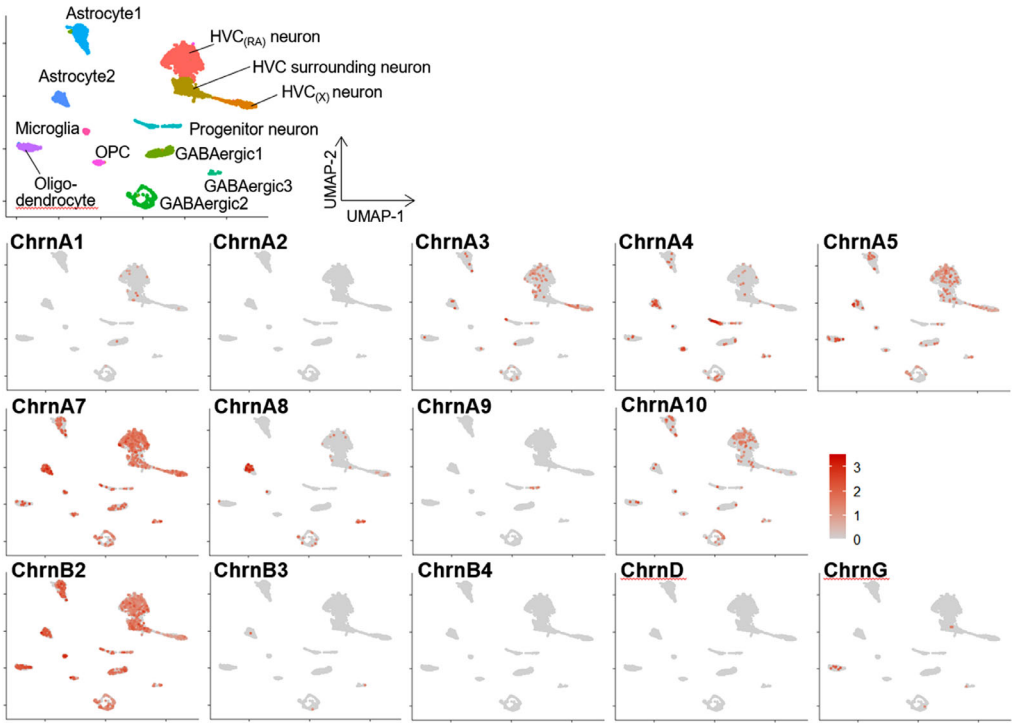

FIGURE 14 Expression of nicotinic acetylcholine receptor (nAChR) subunits in various cell types in HVC. Uniform Manifold Approximation and Projection (UMAP) plots of cells expressing ChrnA1–5, A7–10, B2–4, D, and G in HVC ($n = 6510$ cells). Red dots in each panel represent cells expressing the subunit indicated at the top left. The color gradation represents the intensity of expression. In the reference UMAP panel at the top, each color represents a class of cell types

ChrnB2-expressing cells, ChrnA7 was the main α subunit coexpressed with ChrnB2 in 31%, 66%, and 33% of ChrnB2(+)-$HVC_{(RA)}$, ChrnB2(+)-$HVC_{(X)}$, and ChrnB2(+)-RA projecting neurons, respectively (arrowheads in Figure 17a–c). This information on coexpression suggests the presence of a ChrnA7/B2 heteromeric receptor, which was recently found in rodent and human brains (Liu et al., 2012, 2009; Thomsen et al., 2015). These findings demonstrated that nAChR subunits were expressed in a limited cell population of each cell type in the vocal motor nuclei HVC and RA. Furthermore, nAChR may form ChrnA7-homomeric or ChrnB2-containing heteromeric receptors in these cell populations. However, compared with the more abundant expression of ChrnA7-homomeric receptors, far fewer neuronal cells expressed ChrnB2-containing receptors.

4 | DISCUSSION

To comprehensively investigate the expression of nAChR subunits in an oscine songbird brain, including the neural circuits for acquiring and producing birdsong, we cloned 15 nAChR subunits, ChrnA1–10, B2–4, D, and G, from the zebra finch brain and highlighted their unique expression patterns in the telencephalon, thalamus, midbrain, and cerebellum. Whether the developmental origin of the hyperpallium is distinct or similar to regions below it remains an unsolved problem in avian pallial organization (Jarvis et al., 2005; Medina & Reiner, 2000; Reiner et al., 2004). The results of this study have shown that all six nAChR subunits expressed in the telencephalon were similarly expressed in both the hyperpallium and nidopallium across the mesopallium. The concordant expression of these nAChRs between the hyperpallium and nidopallium is consistent with the hypothesis that these two pallium subdivisions have a common origin (Gedman et al., 2021; Jarvis et al., 2013).

Five of the subunits (ChrnA3–5, A7, and B2) were expressed at varying levels in one or more song nuclei in the zebra finch brain. Of these, only ChrnA5 mRNA was differently regulated in the AFP song nucleus LMAN throughout the critical period of song development. These findings indicated that, in contrast to the change in ACh concentration and the activity of ChAT and AChE in the song nuclei through the critical period of song learning (Sakaguchi & Saito, 1989, 1991), the expression of most nAChR subunits was consistently maintained in the song nuclei during song acquisition. Furthermore, scRNA-seq analysis revealed the potential expression of ChrnA7-homomeric and ChrnB2-containing heteromeric nAChRs in limited cell populations of most neuronal cell types in the vocal premotor nuclei HVC and RA.

4.1 | Comparison of nAChR subunit expression between avian and mammalian species

A similar number of nAChR subunits are expressed in the CNS of avian and mammalian species (Han et al., 2000; Nicolas Le Novere et al.,

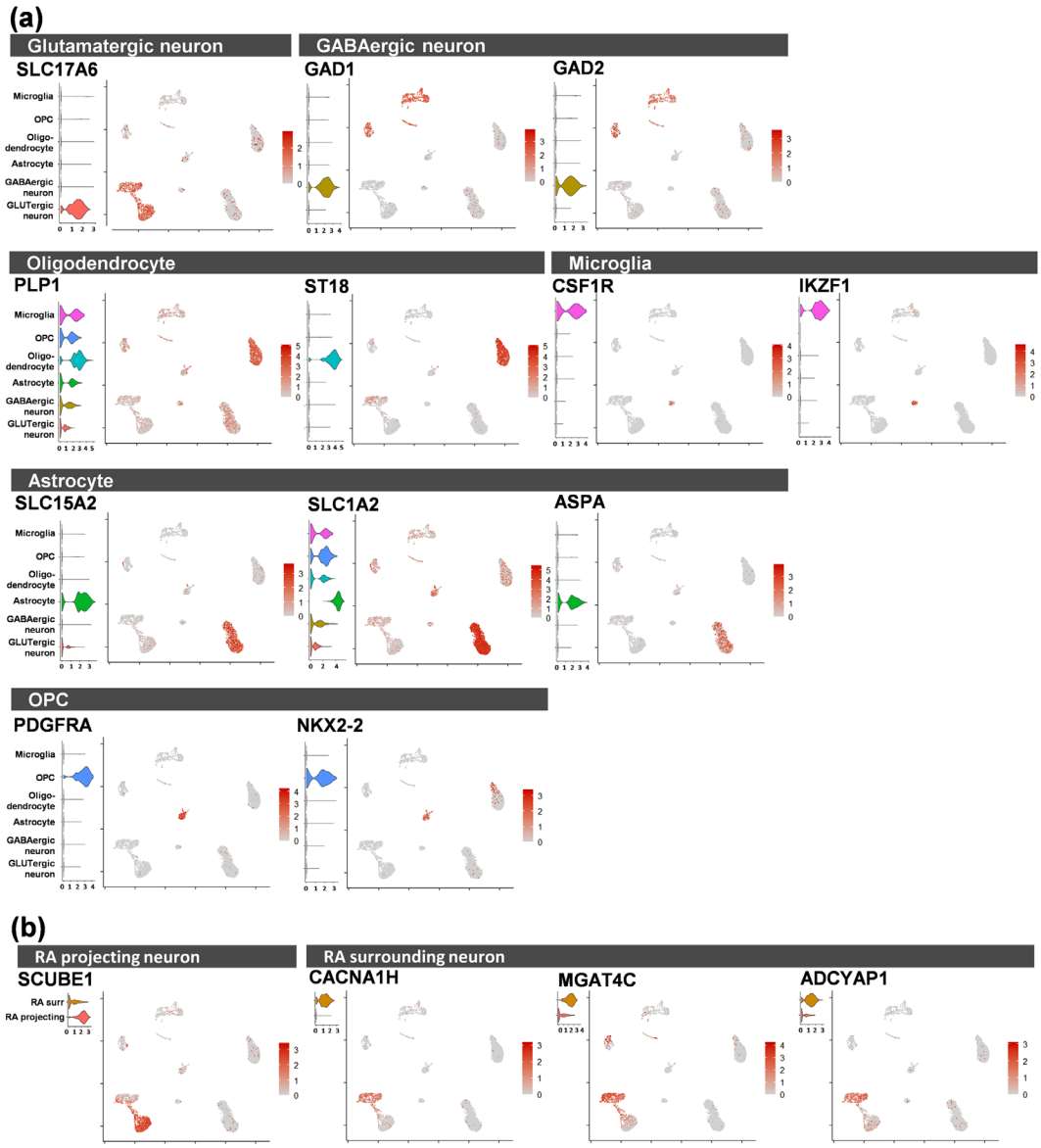

FIGURE 15 Expression of marker genes at each cell-type in RA. Violin (left side panel) and Uniform Manifold Approximation and Projection (UMAP) (right side panel) plots of cell clusters expressing major cell type marker genes (a) and subtype marker of glutamatergic neuron (b)

1996; Lein et al., 2007; Lovell et al., 2018; Morris et al., 1990). However, the expression patterns and levels of nAChRs in the brain are not conserved between them. For example, the pattern of expression of four nAChR subunits (ChrnA1–3, A5) was apparently different in the pallium of zebra finches and the cortex of the mouse (Figures 2–4 and 18). Specifically, ChrnA3 and ChrnA5 were expressed in the mesopallium and entire pallial subregions of the zebra finch, respectively (Figures 2 and 5). In contrast, there was no detectable expression of the mRNAs of these subunits in the mouse cortex (Figure 18). Conversely, ChrnA1 and ChrnA2 were consistently expressed throughout the entire mouse brain, the expression levels of these two α subunits were undetectable in the zebra finch brain. Furthermore, some of the nAChR subunits, such as ChnrA2 and A4, were differentially expressed in the cortical layers of the mice and marmoset (Figure 19), suggesting that nAChRs expression in the telencephalic regions is species-specifically diversified. The discrepancies thus identified in the pattern of expression of nAChR subunits are in sharp contrast to highly conserved expression patterns of the glutamate and dopamine receptor subunits between the avian pallium and mammalian cortical regions (Kubikova et al., 2010; Wada et al., 2004).

4.2 | The potential functional contribution of nAChR subunits in the vocal motor nuclei

Multiple lines of studies in songbirds have suggested potential contributions of the cholinergic system to vocal learning and production.

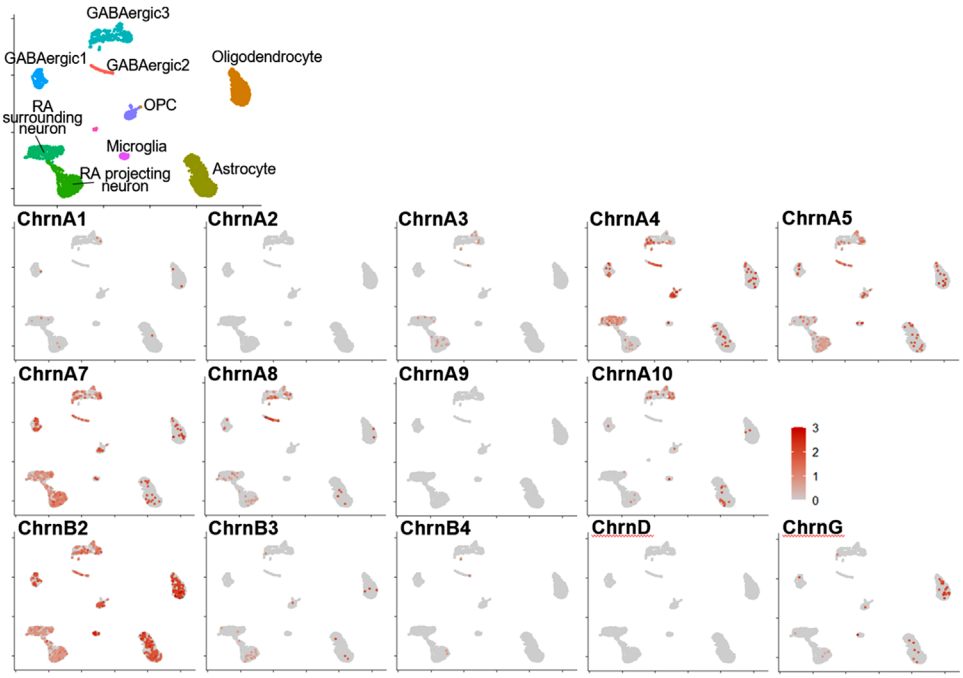

FIGURE 16 Expression of nicotinic acetylcholine receptor (nAChR) subunits in various cell types in RA. Uniform Manifold Approximation and Projection (UMAP) plots of cells expressing ChrnA1–5, A7–10, B2–4, D, and G in RA ($n = 6977$ cells). Red dots in each panel represent cells expressing the subunit indicated at the top left. The color gradation represents the intensity of expression. In the reference UMAP panels (upper), each color represents a class of cell types

For example, stimulating the cholinergic basal forebrain, a region homologous to the nucleus basalis of Meynert in mammals (R. Li & Sakaguchi, 1997; Reiner et al., 2004), suppresses auditory responses to the bird's own song in HVC and RA neurons in anesthetized zebra finches (Shea & Margoliash, 2003). Furthermore, the direct injection of nicotine into HVC produces a strong and consistent suppression of auditory responses in HVC neurons. Arousal state-dependent changes in auditory responses in HVC are an essential modulator of auditory input to the vocal motor region during song learning (Cardin & Schmidt, 2003; Schmidt & Konishi, 1998; Shea & Margoliash, 2003, 2010). However, the precise HVC neuron type responsible for nicotine-induced auditory suppression has not been determined physiologically.

Our scRNA-seq analysis revealed that in HVC, ChrnA3, A5, A7, and B2 were expressed in three neuron types in HVC: $HVC_{(RA)}$ neurons, $HVC_{(X)}$ neurons, and interneurons (Figure 14). However, the populations of cells that expressed these nAChR subunits differed among the neural cell-type classes in HVC. We found that 45% of $HVC_{(RA)}$ neurons and 30% of HVC interneurons expressed at least one type of nAChR subunits, mainly ChrnA7 or B2. In contrast, 77% of $HVC_{(X)}$ neurons expressed one or more of the ChrnA3, A5, A7, and B2 subunits. In particular, 63% of $HVC_{(X)}$ neurons expressed ChrnA7 subunits, which can form functional homomeric receptors. Thus, ChrnA7 subunits may play an important role in modulating the activity of $HVC_{(X)}$ neurons in an arousal state-dependent manner. Further gene manipulation studies of these nAChR subunits at the cell-type level will be crucial to investigate the direct functional contribution of nAChRs in HVC to song learning and production.

In RA, the chronic infusion of a mixture of mAChR and nAChR antagonists during the critical period of song learning induces abnormal song development, characterized by the absence of stereotyped syllable sequences (Puzerey et al., 2018). Acute infusion of the AChR antagonist mixture into RA of juvenile zebra finches does not affect the syllable acoustics or the timing of early plastic songs, suggesting that not cholinergic modulation of fast synaptic transmission but rather cell signaling in RA is crucial for normal song learning (Puzerey et al., 2018). In addition, tetanic stimulation of LMAN to RA axon fibers induces long-term potentiation (LTP) in RA in the presence of nicotine; however, without nicotine it does not produce LTP (Salgado-Commissariat et al., 2004). This nicotine-mediated LTP in RA is blocked by selective antagonists to ChrnA7-homomeric and ChrnA4/B2-heteromeric nAChRs. Our scRNA-seq findings revealed that ChrnA7 was identified in approximately 30% of RA projecting neurons, which could be a sensitive site to ChrnA7 homomeric receptor-specific antagonists in RA. However, although 15% of RA projecting neurons expressed ChrnB2, cells coexpressing ChrnB2 and other α subunits including ChrnA4 accounted for only 0.1%–1.2% of RA projecting neurons. These expression data are contrary to the observed pharmacological effect of ChrnA4/B2 heteromeric nAChR antagonists in RA. Although ChrnA4/B2 coexpression in RA was sparse, we found that 5% of RA projecting neurons coexpressed ChrnA7 and B2. Thus, instead of a

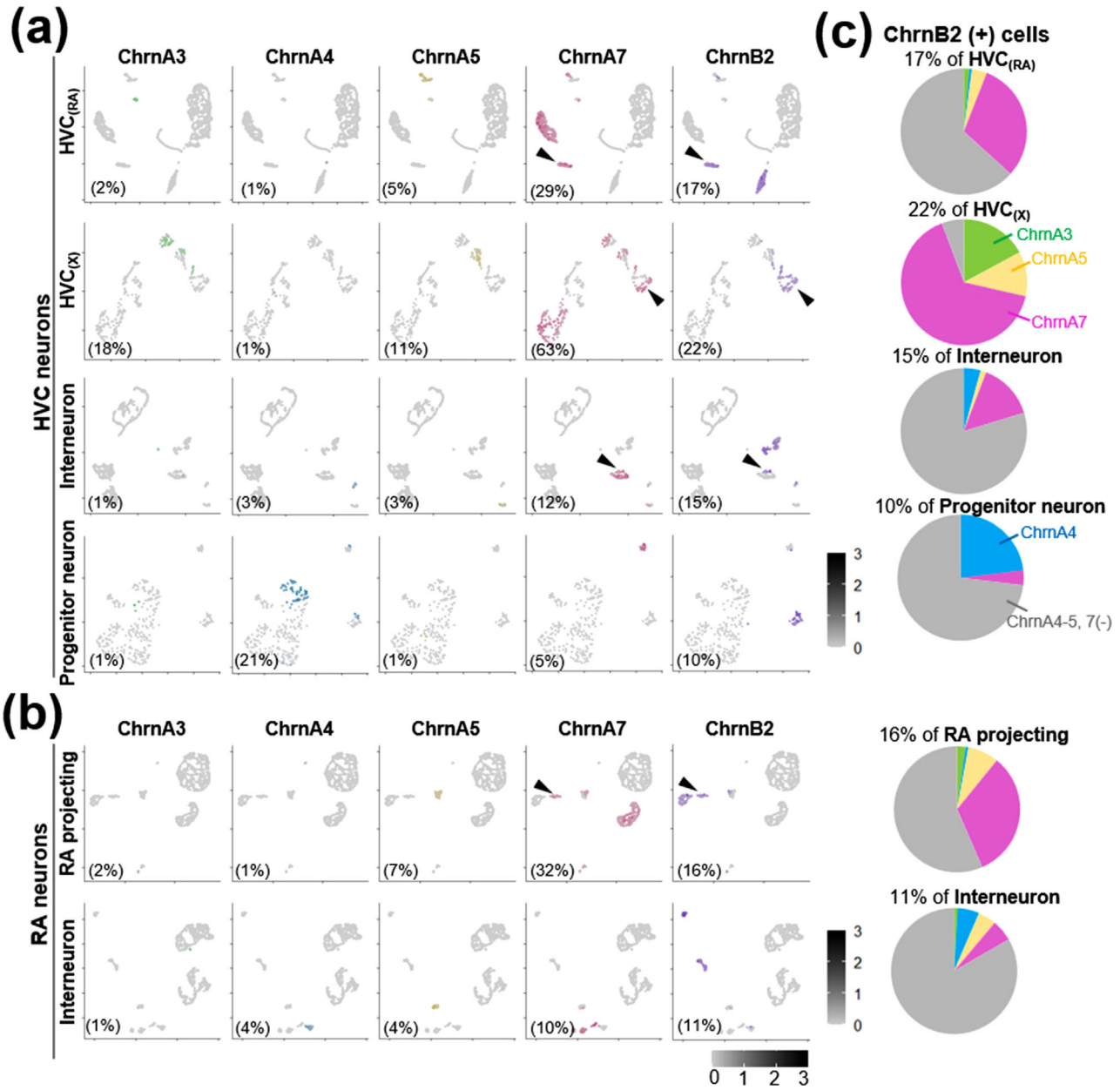

FIGURE 17 Expression of nicotinic acetylcholine receptor (nAChR) subunits in various neuron types in HVC and RA. Uniform Manifold Approximation and Projection (UMAP) plots of neuronal cell types (organized by row) expressing each of the ChrnA3–5, A7, and B2 subunits (organized by column) in HVC (a) and RA (b). Each colored dot represents one neuron expressing the corresponding subunit gene. The color gradation represents the intensity of expression. $HVC_{(RA)}$ and $HVC_{(X)}$ are projecting neurons from HVC to RA and Area X, respectively. $HVC_{(RA)}$, $HVC_{(X)}$, and RA projecting neurons are glutamatergic excitatory neurons. $HVC_{(RA)}$ = 1715 cells; $HVC_{(X)}$ = 326 cells; interneurons in HVC and RA = 896 and 959 cells, respectively; HVC progenitor cells = 275 cells; and RA projecting neurons = 892 cells. Arrowheads indicate cells coexpressing ChrnA7 and B2 subunits. Percentage at the bottom of each UMAP plot is the fraction of the total cell population expressing the corresponding nAChR subunit in the corresponding neural cell type. (c) Coexpression rates of ChrnB2 (+) neurons with ChrnA3 (green), A4 (light blue), A5 (cream-yellow), and A7 (pink). Gray represents negatives (no expression of any of the ChrnA3–5, and A7 subunits

ChrnA4/B2 combination, ChrnA7/B2 heteromeric receptors may contribute to the induction of nicotine-mediated LTP. Notably, approximately half of RA projecting neurons did not express any nAChR subunits. Thus, concerning nAChRs, RA projecting neurons are composed of heterogeneous populations, which may elicit differential responses to nAChR activation by nicotine (Meng et al., 2017; Salgado-Commissariat et al., 2004).

4.3 | The potential functional contribution of nAChR subunits in the AFP nuclei

Similar to the VMP song nuclei, we found that limited nAChR subunits were expressed in the AFP song nuclei, Area X (ChrnA2–5, A7, and B2), aDLM (ChrnA2, A4, A5, A7, and B2), and LMAN (ChrnA2, A5, A7, and B2). Particularly, the expressions of ChrnA5 and B2 were

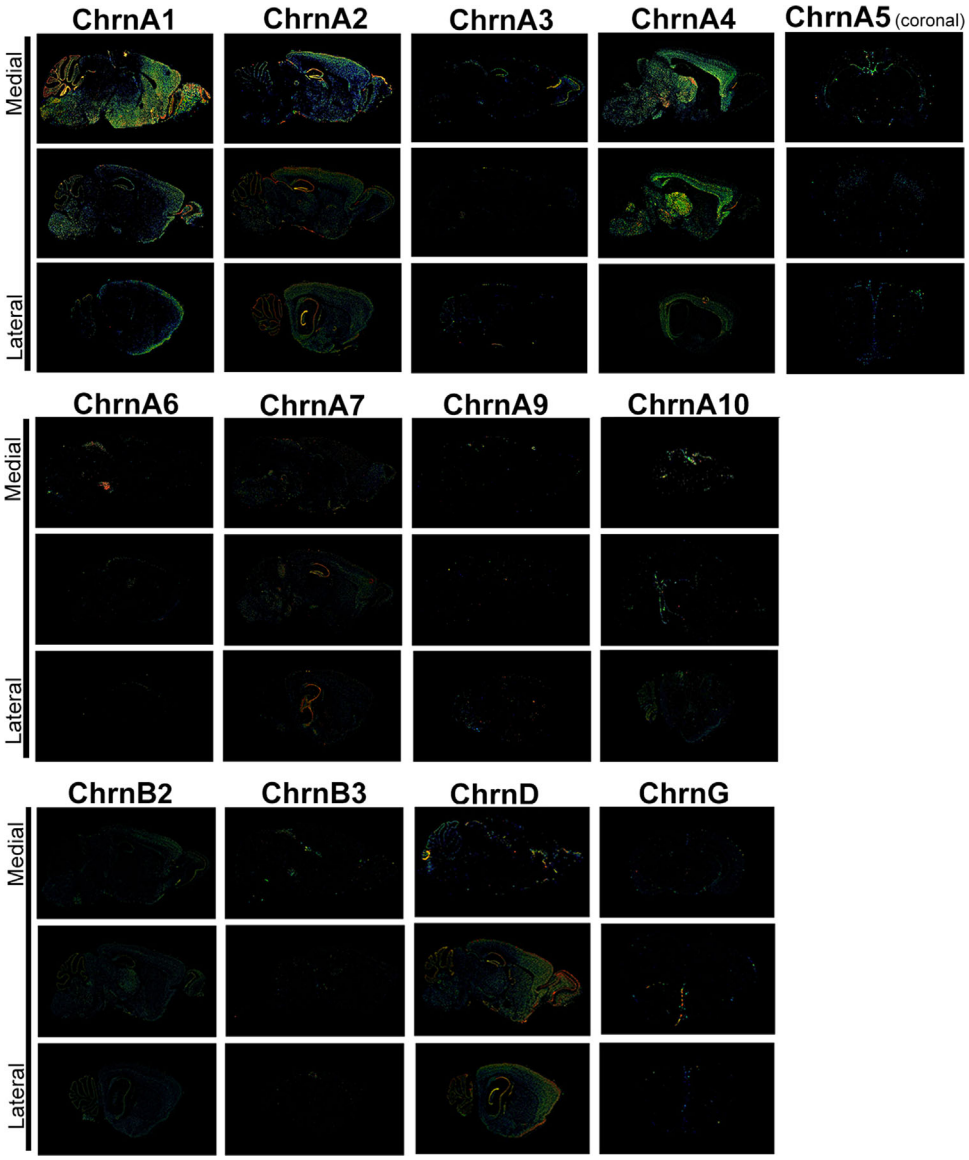

FIGURE 18 Nicotinic acetylcholine receptors (nAChRs) mRNA expression in the mouse brain. All images are adapted from Allen Brain Atlas mouse in situ hybridization data (https://mouse.brain-map.org/search/index)

higher in LMAN than in the surrounding nidopallium. Furthermore, ChrnA5 was the only subunit that showed a significant difference in expression during the critical period of song learning. Although physiological and pharmacological analyses of these subunits have not been performed in the AFP nuclei, our findings suggest that ChrnA7-homomeric and ChrnB2-containing heteromeric nAChRs exist in the AFP song nuclei, as speculated for HVC and RA. The AFP is a crucial neural circuit in the regulation of song learning and maintenance by generating vocal variability (Andalman & Fee, 2009; Aronov et al., 2008; Brainard & Doupe, 2000; Kao et al., 2005; Ölveczky et al., 2005). The concentration of ACh and the activity of ChAT and AChE are increased and maintained in LMAN during the critical period of song learning (Sakaguchi & Saito, 1989, 1991). Thus, specific agonists/antagonists of ChrnA7-homomeric and ChrnB2-containing heteromeric nAChRs could be used to examine whether vocal variability can be modulated during song development. Further studies focusing on particular cell types and nAChR subtype combinations in the song nuclei will be crucial to elucidating cholinergic contributions via the nAChRs involved in neural plasticity and song learning.

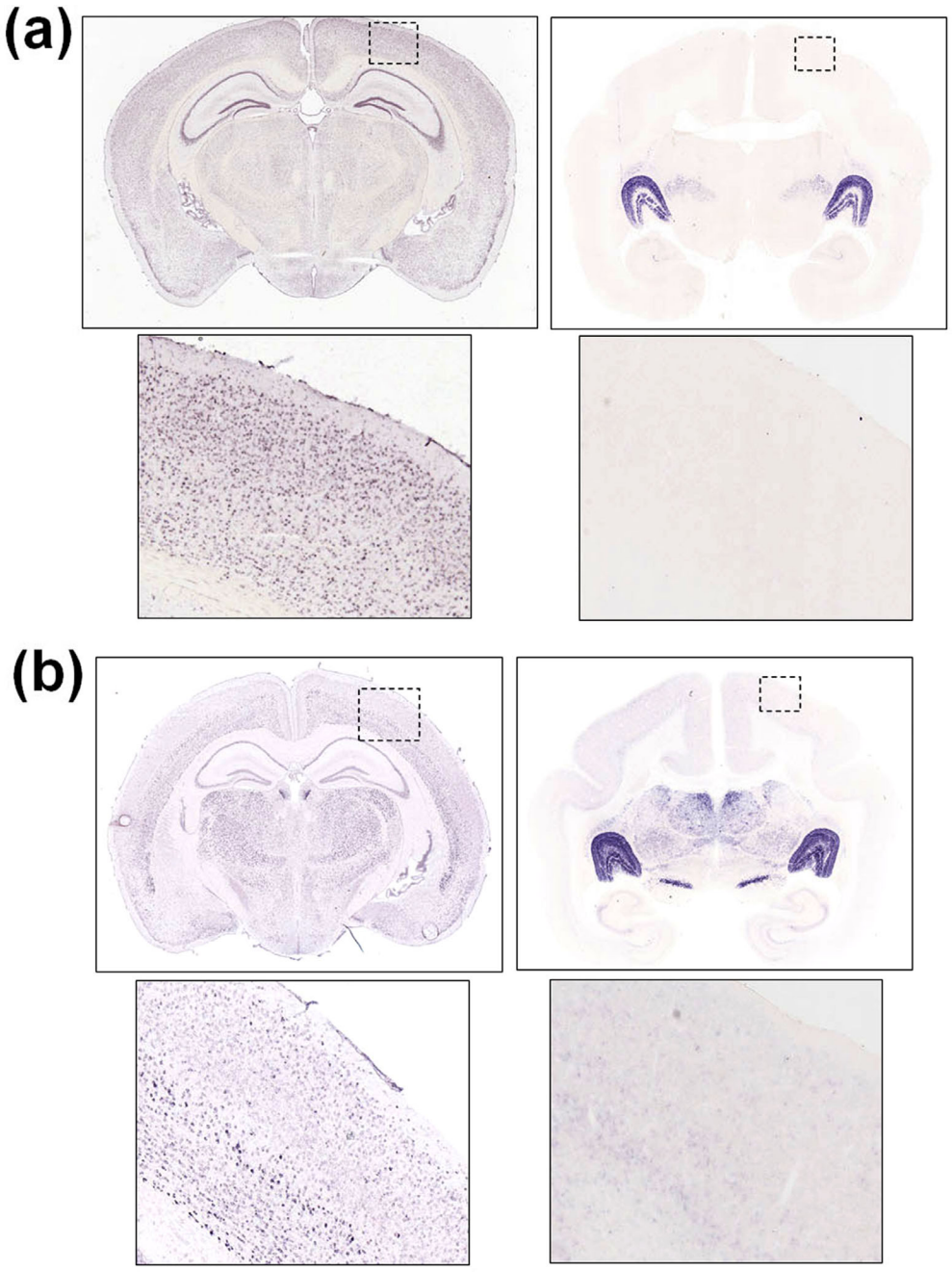

FIGURE 19 Differential expressions of ChrnA2 and A4 between mouse and marmoset cortices. (a) ChrnA2 expression in the mouse (left) and marmoset (right) cortices. (b) ChrnA4 expression in the mouse (left) and marmoset (right) cortices. Panels below are enlarged from enclosed dotted square parts in the above panels. In situ hybridization images are adapted from Allen Brain Atlas mouse ISH data (https://mouse.brain-map.org/search/index) and the Marmoset Gene Atlas (https://gene-atlas.brainminds.riken.jp/)

ACKNOWLEDGMENTS

We appreciate Mrs. Keiko Sumida for her great contribution toward breeding our experimental birds. This research was supported by Japan Studnet Services Organization (JASSO): Follow-up Research Fellowship:153033 to Norman Chinweike Asogwa, and MEXT/JSPS KAKENHI Grant Number 4903-JP17H06380, JP19H04888, JP21H02456, JP21K18265, and the Takeda Science Foundation to Kazuhiro Wada.

CONFLICT OF INTEREST

The authors declare no conflict of interest.

AUTHOR CONTRIBUTIONS

Norman Chinweike Asogwa, Noriyuki Toji, and Kazuhiro Wada designed the research. Norman Chinweike Asogwa, Noriyuki Toji, Ziwei He, and Kazuhiro Wada performed the experiments. Norman Chinweike Asogwa, Noriyuki Toji, and Kazuhiro Wada performed

the analysis. Chengru Shao, Yukino Shibata, Shoji Tatsumoto, Hiroe Ishikawa, and Yasuhiro Go contributed to critical support for experiments and analysis. Norman Chinweike Asogwa, Noriyuki Toji, and Kazuhiro Wada wrote the manuscript. All authors read and approved the final manuscript.

DATA AVAILABILITY STATEMENT

The authors confirm that all of the data underlying the reported findings are included in the manuscript. All raw data are available from the corresponding author on request.

PEER REVIEW

The peer review history for this article is available at https://publons.com/publon/10.1002/cne.25314.

ORCID

Kazuhiro Wada https://orcid.org/0000-0001-8137-9144

REFERENCES

Albuquerque, E. X., Pereira, E. F., Alkondon, M., & Rogers, S. W. (2009). Mammalian nicotinic acetylcholine receptors: From structure to function. *Physiological Reviews*, *89*(1), 73–120. https://doi.org/10.1152/physrev.00015.2008

Anagnostaras, S. G., Murphy, G. G., Hamilton, S. E., Mitchell, S. L., Rahnama, N. P., Nathanson, N. M., & Silva, A. J. (2003). Selective cognitive dysfunction in acetylcholine M1 muscarinic receptor mutant mice. *Nature Neuroscience*, *6*(1), 51–58. https://doi.org/10.1038/nn992

Andalman, A. S., & Fee, M. S. (2009). A basal ganglia-forebrain circuit in the songbird biases motor output to avoid vocal errors. *Proceedings of the National Academy of Sciences*, *106*(30), 12518–12523. https://doi.org/10.1073/pnas.0903214106

Aronov, D., Andalman, A. S., & Fee, M. S. (2008). A specialized forebrain circuit for vocal babbling in the juvenile songbird. *Science*, *320*(5876), 630–634. https://doi.org/10.1126/science.1155140

Aronov, D., Veit, L., Goldberg, J. H., & Fee, M. S. (2011). Two distinct modes of forebrain circuit dynamics underlie temporal patterning in the vocalizations of young songbirds. *Journal of Neuroscience*, *31*(45), 16353–16368. https://doi.org/10.1523/JNEUROSCI.3009-11.2011

Asogwa, N. C., Mori, C., Sanchez-Valpuesta, M., Hayase, S., & Wada, K. (2018). Inter- and intra-specific differences in muscarinic acetylcholine receptor expression in the neural pathways for vocal learning in songbirds. *Journal of Comparative Neurology*, *526*(17), 2856–2869. https://doi.org/10.1002/cne.24532

Bell, Z. W., Lovell, P., Mello, C. V., Yip, P. K., George, J. M., & Clayton, D. F. (2019). Urotensin-related gene transcripts mark developmental emergence of the male forebrain vocal control system in songbirds. *Science Reports*, *9*(1), 816. https://doi.org/10.1038/s41598-018-37057-w

Boord, R. L. (1968). Ascending projections of the primary cochlear nuclei and nucleus laminaris in the pigeon. *Journal of Comparative Neurology*, *133*(4), 523–541. https://doi.org/10.1002/cne.901330410

Bottjer, S. W., & Altenau, B. (2010). Parallel pathways for vocal learning in basal ganglia of songbirds. *Nature Neuroscience*, *13*(2), 153–155. https://doi.org/10.1038/nn.2472

Bottjer, S. W., Miesner, E. A., & Arnold, A. P. (1984). Forebrain lesions disrupt development but not maintenance of song in passerine birds. *Science*, *224*(4651), 901–903. https://doi.org/10.1126/science.6719123

Brainard, M. S., & Doupe, A. J. (2000). Interruption of a basal ganglia-forebrain circuit prevents plasticity of learned vocalizations. *Nature*, *404*(6779), 762–766. https://doi.org/10.1038/35008083

Brenowitz, E. A., & Beecher, M. D. (2005). Song learning in birds: Diversity and plasticity, opportunities and challenges. *Trends in Neuroscience*, *28*(3), 127–132. https://doi.org/10.1016/j.tins.2005.01.004

Cardin, J. A., & Schmidt, M. F. (2003). Song system auditory responses are stable and highly tuned during sedation, rapidly modulated and unselective during wakefulness, and suppressed by arousal. *Journal of Neurophysiology*, *90*(5), 2884–2899. https://doi.org/10.1152/jn.00391.2003

Colquitt, B. M., Merullo, D. P., Konopka, G., Roberts, T. F., & Brainard, M. S. (2021). Cellular transcriptomics reveals evolutionary identities of songbird vocal circuits. *Science*, *371*(6530), 676–677. https://doi.org/10.1126/science.abd9704

Conner, J. M., Culberson, A., Packowski, C., Chiba, A. A., & Tuszynski, M. H. (2003). Lesions of the basal forebrain cholinergic system impair task acquisition and abolish cortical plasticity associated with motor skill learning. *Neuron*, *38*(5), 819–829. https://doi.org/10.1016/S0896-6273(03)00288-5

Couturier, S., Bertrand, D., Matter, J.-M., Hernandez, M.-C., Bertrand, S., Millar, N., Valera, S., Barkas, T., & Ballivet, M. (1990). A neuronal nicotinic acetylcholine receptor subunit (α7) is developmentally regulated and forms a homo-oligomeric channel blocked by α-BTX. *Neuron*, *5*(6), 847–856. https://doi.org/10.1016/0896-6273(90)90344-F

Dajas-Bailador, F., & Wonnacott, S. (2004). Nicotinic acetylcholine receptors and the regulation of neuronal signalling. *Trends in Pharmacological Sciences*, *25*(6), 317–324. https://doi.org/10.1016/j.tips.2004.04.006

Dineley-Miller, K., & Patrick, J. (1992). Gene transcripts for the nicotinic acetylcholine receptor subunit, beta4, are distributed in multiple areas of the rat central nervous system. *Molecular Brain Research*, *16*(3), 339–344. https://doi.org/10.1016/0169-328X(92)90244-6

Doupe, A. J., & Kuhl, P. K. (1999). Birdsong and human speech: Common themes and mechanisms. *Annual Review of Neuroscience*, *22*, 567–631. https://doi.org/10.1146/annurev.neuro.22.1.567

Fu, Y., Tucciarone, J. M., Espinosa, J. S., Sheng, N., Darcy, D. P., Nicoll, R. A., Josh Huang, Z., & Stryker, M. P. (2014). A cortical circuit for gain control by behavioral state. *Cell*, *156*(6), 1139–1152. https://doi.org/10.1016/j.cell.2014.01.050

Gedman, G., Haase, B., Durieux, G., Biegler, M. T., Fedrigo, O., & Jarvis, E. D. (2021). As above, so below: Whole transcriptome profiling demonstrates strong molecular similarities between avian dorsal and ventral pallial subdivisions. *Journal of Comparative Neurology*, *529*(12), 3222–3246. https://doi.org/10.1002/cne.25159

Gotti, C., & Clementi, F. (2004). Neuronal nicotinic receptors: From structure to pathology. *Progress in Neurobiology*, *74*(6), 363–396. https://doi.org/10.1016/j.pneurobio.2004.09.006

Gotti, C., Clementi, F., Fornari, A., Gaimarri, A., Guiducci, S., Manfredi, I., Moretti, M., Pedrazzi, P., Pucci, L., & Zoli, M. (2009). Structural and functional diversity of native brain neuronal nicotinic receptors. *Biochemical Pharmacology*, *78*(7), 703–711. https://doi.org/10.1016/j.bcp.2009.05.024

Halvorsen, S. W., & Berg, D. K. (1990). Subunit composition of nicotinic acetylcholine receptors from chick ciliary ganglia. *Journal of Neuroscience*, *10*(6), 1711–1718. https://doi.org/10.1523/JNEUROSCI.10-06-01711.1990

Han, Z.-Y., Le Novère, N., Zoli, M., Hill, Jr, J. A., Champtiaux, N., & Changeux, J.-P. (2000). Localization of nAChR subunit mRNAs in the brain of Macaca mulatta. *European Journal of Neuroscience*, *12*(10), 3664–3674. https://doi.org/10.1046/j.1460-9568.2000.00262.x

Hasselmo, M. E. (2006). The role of acetylcholine in learning and memory. *Current Opinion in Neurobiology*, *16*(6), 710–715. https://doi.org/10.1016/j.conb.2006.09.002

Herrero, J. L., Roberts, M. J., Delicato, L. S., Gieselmann, M. A., Dayan, P., & Thiele, A. (2008). Acetylcholine contributes through muscarinic receptors to attentional modulation in V1. *Nature*, *454*(7208), 1110–1114. https://doi.org/10.1038/nature07141

Jarvis, E. D., Gunturkun, O., Bruce, L., Csillag, A., Karten, H., Kuenzel, W., Lee, D. W., Medina, L., Paxinos, G., Perkel, D. J., Shimizu, T., Striedter, G., Wild, J. M., Ball, G. F., Dugas-Ford, J., Durand, S. E., Hough, G. E., Husband, S., Kubikova, L., Lee, D. W., … Butler, A. B. (2005). Avian brains and

a new understanding of vertebrate brain evolution. *Nature Reviews Neuroscience*, *6*(2), 151–159. https://doi.org/10.1038/nrn1606

Jarvis, E. D., Yu, J., Rivas, M. V., Horita, H., Feenders, G., Whitney, O., Jarvis, S. C., Jarvis, E. R., Kubikova, L., Puck, A. E. P., Siang-Bakshi, C., Martin, S., Mcelroy, M., Hara, E., Howard, J., Pfenning, A., Mouritsen, H., Chen, C.-C., & Wada, K. (2013). Global view of the functional molecular organization of the avian cerebrum: Mirror images and functional columns. *Journal of Comparative Neurology*, *521*(16), 3614–3665. https://doi.org/10.1002/cne.23404

Kao, M. H., Doupe, A. J., & Brainard, M. S. (2005). Contributions of an avian basal ganglia-forebrain circuit to real-time modulation of song. *Nature*, *433*(7026), 638–643. https://doi.org/10.1038/nature03127

Kruse, A. C., Kobilka, B. K., Gautam, D., Sexton, P. M., Christopoulos, A., & Wess, J. (2014). Muscarinic acetylcholine receptors: Novel opportunities for drug development. *Nature Reviews Drug Discovery*, *13*(7), 549–560. https://doi.org/10.1038/nrd4295

Kubikova, L., Wada, K., & Jarvis, E. D. (2010). Dopamine receptors in a songbird brain. *Journal of Comparative Neurology*, *518*(6), 741–769. https://doi.org/10.1002/cne.22255

Le Novere, N., Corringer, P. J., & Changeux, J. P. (2002). The diversity of subunit composition in nAChRs: Evolutionary origins, physiologic and pharmacologic consequences. *Journal of Neurobiology*, *53*(4), 447–456. https://doi.org/10.1002/neu.10153

Le Novere, N., Zoli, M., & Changeux, J. P. (1996). Neuronal nicotinic receptor a6 subunit mRNA is selectively concentrated in catecholaminergic nuclei of the rat brain. *European Journal of Neuroscience*, *8*(11), 2428–2439. https://doi.org/10.1111/j.1460-9568.1996.tb01206.x

Lein, E. S., Hawrylycz, M. J., Ao, N., Ayres, M., Bensinger, A., Bernard, A., Boe, A. F., Boguski, M. S., Brockway, K. S., Byrnes, E. J., Chen, L., Chen, L., Cheng, T.-M., Chin, C. M., Chong, J., Crook, B. E., Czaplinska, A., Dang, C. N., Datta, S., … Jones, A. R. (2007). Genome-wide atlas of gene expression in the adult mouse brain. *Nature*, *445*(7124), 168–176. https://doi.org/10.1038/nature05453

Li, H. Q., & Spitzer, N. C. (2020). Exercise enhances motor skill learning by neurotransmitter switching in the adult midbrain. *Nature Communication*, *11*(1), 2195. https://doi.org/10.1038/s41467-020-16053-7

Li, R., & Sakaguchi, H. (1997). Cholinergic innervation of the song control nuclei by the ventral paleostriatum in the zebra finch: A double-labeling study with retrograde fluorescent tracers and choline acetyltransferase immunohistochemistry. *Brain Research*, *763*(2), 239–246. https://doi.org/10.1016/S0006-8993(97)00417-4

Liu, Q., Huang, Y., Shen, J., Steffensen, S., & Wu, J. (2012). Functional $\alpha 7\beta 2$ nicotinic acetylcholine receptors expressed in hippocampal interneurons exhibit high sensitivity to pathological level of amyloid β peptides. *BMC Neuroscience*, *13*(1), 155. https://doi.org/10.1186/1471-2202-13-155

Liu, Q., Huang, Y., Xue, F., Simard, A., DeChon, J., Li, G., Zhang, J., Lucero, L., Wang, M., Sierks, M., Hu, G., Chang, Y., Lukas, R. J., & Wu, J. (2009). A novel nicotinic acetylcholine receptor subtype in basal forebrain cholinergic neurons with high sensitivity to amyloid peptides. *Journal of Neuroscience*, *29*(4), 918–929. https://doi.org/10.1523/JNEUROSCI.3952-08.2009

Lovell, P. V., Clayton, D. F., Replogle, K. L., & Mello, C. V. (2008). Birdsong "transcriptomics": Neurochemical specializations of the oscine song system. *PLoS One*, *3*(10), e3440. https://doi.org/10.1371/journal.pone.0003440

Lovell, P. V., Huizinga, N. A., Friedrich, S. R., Wirthlin, M., & Mello, C. V. (2018). The constitutive differential transcriptome of a brain circuit for vocal learning. *BMC Genomics*, *19*(1), 231. https://doi.org/10.1186/s12864-018-4578-0

Lovell, P. V., Wirthlin, M., Kaser, T., Buckner, A. A., Carleton, J. B., Snider, B. R., McHugh, A. K., Tolpygo, A., Mitra, P. P., & Mello, C. V. (2020). ZEBrA: Zebra finch Expression Brain Atlas-A resource for comparative molecular neuroanatomy and brain evolution studies. *Journal of Comparative Neurology*, *528*(12), 2099–2131. https://doi.org/10.1002/cne.24879

Luo, M., Ding, L., & Perkel, D. J. (2001). An avian basal ganglia pathway essential for vocal learning forms a closed topographic loop. *Journal of Neuroscience*, *21*(17), 6836–6845. https://doi.org/10.1523/JNEUROSCI.21-17-06836.2001

Marler, P., & Slabbekoorn, H. (2004). *Nature's music: The science of birdsong*. Elsevier Academic Press.

Medina, L., & Reiner, A. (2000). Do birds possess homologues of mammalian primary visual, somatosensory and motor cortices? *Trends in Neuroscience„ 23*(1), 1–12. https://doi.org/10.1016/S0166-2236(99)01486-1

Mello, C. V., Kaser, T., Buckner, A. A., Wirthlin, M., & Lovell, P. V. (2019). Molecular architecture of the zebra finch arcopallium. *Journal of Comparative Neurology*, *527*, 2512–2556. https://doi.org/10.1002/cne.24688

Meng, W., Wang, S., Yao, L., Zhang, N., & Li, D. (2017). Muscarinic receptors are responsible for the cholinergic modulation of projection neurons in the song production brain nucleus RA of zebra finches. *Frontiers in Cellular Neuroscience*, *11*, 51. https://doi.org/10.3389/fncel.2017.00051

Morris, B. J., Hicks, A. A., Wisden, W., Darlison, M. G., Hunt, S. P., & Barnard, E. A. (1990). Distinct regional expression of nicotinic acetylcholine receptor genes in chick brain. *Molecular Brain Research*, *7*(4), 305–315. https://doi.org/10.1016/0169-328X(90)90081-N

Nottebohm, F., Stokes, T. M., & Leonard, C. M. (1976). Central control of song in the canary, *Serinus canarius*. *Journal of Comparative Neurology*, *165*(4), 457–486. https://doi.org/10.1002/cne.901650405

Noudoost, B., & Moore, T. (2011). The role of neuromodulators in selective attention. *Trends in Cognitive Sciences*, *15*(12), 585–591. https://doi.org/10.1016/j.tics.2011.10.006

Ölveczky, B. P., Andalman, A. S., & Fee, M. S. (2005). Vocal experimentation in the juvenile songbird requires a basal ganglia circuit. *PLoS Biology*, *3*(5), e153. https://doi.org/10.1371/journal.pbio.0030153.g001

Parikh, V., Kozak, R., Martinez, V., & Sarter, M. (2007). Prefrontal acetylcholine release controls cue detection on multiple timescales. *Neuron*, *56*(1), 141–154. https://doi.org/10.1016/j.neuron.2007.08.⟨?PMU?⟩025

Pedersen, J. E., Bergqvist, C. A., & Larhammar, D. (2019). Evolution of vertebrate nicotinic acetylcholine receptors. *BMC Evolutionary Biology*, *19*(1), 38. https://doi.org/10.1186/s12862-018-1341-8

Puzerey, P. A., Maher, K., Prasad, N., & Goldberg, J. H. (2018). Vocal learning in songbirds requires cholinergic signaling in a motor cortex-like nucleus. *Journal of Neurophysiology*, *120*(4), 1796–1806. https://doi.org/10.1152/jn.00078.2018

Ramon y Cajal, S. (1911). Histologie du système nerveux de l'homme et des vertébrés. *Maloine, Paris*, *2*, 153–173.

Reiner, A., Perkel, D. J., Bruce, L. L., Butler, A. B., Csillag, A., Kuenzel, W., Medina, L., Paxinos, G., Shimizu, T., Striedter, G., Wild, M., Ball, G. F., Durand, S., Gütürkün, O., Lee, D. W., Mello, C. V., Powers, A., White, S. A., Hough, G., … Avian Brain Nomenclature, F. (2004). Revised nomenclature for avian telencephalon and some related brainstem nuclei. *Journal of Comparative Neurology*, *473*(3), 377–414. https://doi.org/10.1002/cne.20118

Role, L. W., & Berg, D. K. (1996). Nicotinic receptors in the development and modulation of CNS synapses. *Neuron*, *16*(6), 1077–1085. https://doi.org/10.1016/S0896-6273(00)80134-8

Ryan, S. M., & Arnold, A. P. (1981). Evidence for cholinergic participation in the control of bird song; acetylcholinesterase distribution and muscarinic receptor autoradiography in the zebra finch brain. *Journal of Comparative Neurology*, *202*(2), 211–219. https://doi.org/10.1002/cne.902020207

Sadananda, M. (2004). Acetylcholinesterase in central vocal control nuclei of the zebra finch (*Taeniopygia guttata*). *Journal of Biosciences*, *29*(2), 189–200. https://doi.org/10.1007/BF02703417

Sakaguchi, H., & Saito, N. (1989). The acetylcholine and catecholamine contents in song control nuclei of zebra finch during song ontogeny. *Developmental Brain Research*, *47*(2), 313–317. https://doi.org/10.1016/0165-3806(89)90189-2

Sakaguchi, H., & Saito, N. (1991). Developmental change of cholinergic activity in the forebrain of the zebra finch during song learning. *Developmental Brain Research*, *62*(2), 223–228. https://doi.org/10.1016/0165-3806(91)90169-J

Salgado-Commissariat, D., Rosenfield, D. B., & Helekar, S. A. (2004). Nicotine-mediated plasticity in robust nucleus of the archistriatum of the adult zebra finch. *Brain Research*, *1018*(1), 97–105. https://doi.org/10.1016/j.brainres.2004.05.051

Sargent, P. B. (1993). The diversity of neuronal nicotinic acetylcholine receptors. *Annual Review of Neuroscience*, *16*(1), 403–443. https://doi.org/10.1146/annurev.ne.16.030193.002155

Sarter, M., Bruno, J. P., & Turchi, J. (1999). Basal forebrain afferent projections modulating cortical acetylcholine, attention, and implications for neuropsychiatric disorders. *Annals of the New York Academy of Sciences*, *877*, 368–382. https://doi.org/10.1111/j.1749-6632.1999.tb09277.x

Saunders, A., Macosko, E. Z., Wysoker, A., Goldman, M., Krienen, F. M., de Rivera, H., Bien, E., Baum, M., Bortolin, L., Wang, S., Goeva, A., Nemesh, J., Kamitaki, N., Brumbaugh, S., Kulp, D., & McCarroll, S. A. (2018). Molecular diversity and specializations among the cells of the adult mouse brain. *Cell*, *174*(4), 1015–1030. https://doi.org/10.1016/j.cell.2018.07.028

Scharff, C., & Nottebohm, F. (1991). A comparative study of the behavioral deficits following lesions of various parts of the zebra finch song system: Implications for vocal learning. *Journal of Neuroscience*, *11*(9), 2896–2913. https://doi.org/10.1523/JNEUROSCI.11-09-02896.1991

Schmidt, M. F., & Konishi, M. (1998). Gating of auditory responses in the vocal control system of awake songbirds. *Nature Neuroscience*, *1*(6), 513. https://doi.org/10.1038/2232

Schryver, H. M., & Mysore, S. P. (2019). Spatial dependence of stimulus competition in the avian nucleus isthmi pars magnocellularis. *Brain Behavior and Evolution*, *93*(2–3), 137–151. https://doi.org/10.1159/000500192

Scully, E. N., Acerbo, M. J., & Lazareva, O. F. (2014). Bilateral lesions of nucleus subpretectalis/interstitio-pretecto-subpretectalis (SP/IPS) selectively impair figure-ground discrimination in pigeons. *Visual Neuroscience*, *31*(1), 105–110. https://doi.org/10.1017/S0952523813000424

Shea, S. D., Koch, H., Baleckaitis, D., Ramirez, J. M., & Margoliash, D. (2010). Neuron-specific cholinergic modulation of a forebrain song control nucleus. *Journal of Neurophysiology*, *103*(2), 733–745. https://doi.org/10.1152/jn.00803.2009

Shea, S. D., & Margoliash, D. (2003). Basal forebrain cholinergic modulation of auditory activity in the zebra finch song system. *Neuron*, *40*(6), 1213–1226. https://doi.org/10.1016/S0896-6273(03)00723-2

Shea, S. D., & Margoliash, D. (2010). Behavioral state-dependent reconfiguration of song-related network activity and cholinergic systems. *Journal of Chemical Neuroanatomy*, *39*(2), 132–140. https://doi.org/10.1016/j.jchemneu.2009.10.002

Stuart, T., Butler, A., Hoffman, P., Hafemeister, C., Papalexi, E., Mauck, W. M. 3rd, Hao, Y., Stoeckius, M., Smibert, P., & Satija, R. (2019). Comprehensive integration of single-cell data. *Cell*, *177*(7), 1888–1902. https://doi.org/10.1016/j.cell.2019.05.031

Tasic, B., Menon, V., Nguyen, T. N., Kim, T. K., Jarsky, T., Yao, Z., Levi, B., Gray, L. T., Sorensen, S. A., Dolbeare, T., Bertagnolli, D., Goldy, J., Shapovalova, N., Parry, S. Lee, C., Smith, K., Bernard, A., Madisen, L., Sunkin, S. M., … Zeng, H. (2016). Adult mouse cortical cell taxonomy revealed by single cell transcriptomics. *Nature Neuroscience*, *19*(2), 335–346. https://doi.org/10.1038/nn.4216

Tasic, B., Yao, Z., Graybuck, L. T., Smith, K. A., Nguyen, T. N., Bertagnolli, D., Goldy, J., Garren, E., Economo, M. N., Viswanathan, S., Penn, O., Bakken, T., Menon, V., Miller, J., Fong, O., Hirokawa, K. E., Lathia, K., Rimorin, C., Tieu, M., … Zeng, H. (2018). Shared and distinct transcriptomic cell types across neocortical areas. *Nature*, *563*(7729), 72–78. https://doi.org/10.1038/s41586-018-0654-5

Thomsen, M. S., Zwart, R., Ursu, D., Jensen, M. M., Pinborg, L. H., Gilmour, G., Wu, J., Sher, E., & Mikkelsen, J. D. (2015). Alpha7 and beta2 nicotinic acetylcholine receptor subunits form heteromeric receptor complexes that are expressed in the human cortex and display distinct pharmacological properties. *PLoS One*, *10*(6), e0130572. https://doi.org/10.1371/journal.pone.0130572

Thouvarecq, R., Protais, P., Jouen, F., & Caston, J. (2001). Influence of cholinergic system on motor learning during aging in mice. *Behavioural Brain Research*, *118*(2), 209–218. https://doi.org/10.1016/S0166-4328(00)00330-2

Wada, K., Ballivet, M., Boulter, J., Connolly, J., Wada, E., Deneris, E. S., Swanson, L. W., Heinemann, S., & Patrick, J. (1988). Functional expression of a new pharmacological subtype of brain nicotinic acetylcholine receptor. *Science*, *240*(4850), 330–334. https://doi.org/10.1126/science.2832952

Wada, K., Sakaguchi, H., Jarvis, E. D., & Hagiwara, M. (2004). Differential expression of glutamate receptors in avian neural pathways for learned vocalization. *Journal of Comparative Neurology*, *476*(1), 44–64. https://doi.org/10.1002/cne.20201

Wallace, T. L., & Bertrand, D. (2013). Importance of the nicotinic acetylcholine receptor system in the prefrontal cortex. *Biochemical Pharmacology*, *85*(12), 1713–1720. https://doi.org/10.1016/j.bcp.2013.04.001

Watson, J. T., Adkins-Regan, E., Whiting, P., Lindstrom, J. M., & Podleski, T. R. (1988). Autoradiographic localization of nicotinic acetylcholine receptors in the brain of the zebra finch (Poephila guttata). *Journal of Comparative Neurology*, *274*(2), 255–264. https://doi.org/10.1002/cne.902740209

Whiting, P., Schoepfer, R., Conroy, W., Gore, M., Keyser, K., Shimasaki, S., Esch, F., & Lindstrom, J. (1991). Expression of nicotinic acetylcholine receptor subtypes in brain and retina. *Molecular Brain Research*, *10*(1), 61–70. https://doi.org/10.1016/0169-328X(91)90057-5

Winzer-Serhan, U. H., & Leslie, F. M. (1997). Codistribution of nicotinic acetylcholine receptor subunit $\alpha 3$ and $\beta 4$ mRNAs during rat brain development. *Journal of Comparative Neurology*, *386*(4), 540–554. https://doi.org/10.1002/(SICI)1096-9861(19971006)386:4<540::AID-CNE2>3.0.CO;2-2

Wonnacott, S. (1997). Presynaptic nicotinic ACh receptors. *Trends in Neuroscience (Tins)*, *20*(2), 92–98. https://doi.org/10.1016/S0166-2236(96)10073-4

Woolley, S. M., & Portfors, C. V. (2013). Conserved mechanisms of vocalization coding in mammalian and songbird auditory midbrain. *Hearing Research*, *305*, 45–56. https://doi.org/10.1016/j.heares.2013.05.005

Wylie, D. R., Gutierrez-Ibanez, C., Pakan, J. M., & Iwaniuk, A. N. (2009). The optic tectum of birds: Mapping our way to understanding visual processing. *Canadian Journal of Experimental Psychology*, *63*(4), 328–338. https://doi.org/10.1037/a0016826

Zhang, Y., Chen, K., Sloan, S. A., Bennett, M. L., Scholze, A. R., O'Keeffe, S., Phatnani, H. P., Guarnieri, P., Caneda, C., Ruderisch, N., Deng, S., Liddelow, S. A., Zhang, C., Daneman, R., Maniatis, T., Barres, B. A., & Wu, J. Q. (2014). An RNA-sequencing transcriptome and splicing database of glia, neurons, and vascular cells of the cerebral cortex. *Journal of Neuroscience*, *34*(36), 11929–11947. https://doi.org/10.1523/JNEUROSCI.1860-14.2014

Zoli, M., Le Novere, N., Hill, J. A., & Changeux, J.-P. (1995). Developmental regulation of nicotinic ACh receptor subunit mRNAs in the rat central and peripheral nervous systems. *Journal of Neuroscience*, *15*(3), 1912–1939. https://doi.org/10.1523/JNEUROSCI.15-03-01912.1995

Zoli, M., Pistillo, F., & Gotti, C. (2015). Diversity of native nicotinic receptor subtypes in mammalian brain. *Neuropharmacology*, *96*(Pt B), 302–311. https://doi.org/10.1016/j.neuropharm.2014.11.003

Zoli, M., Pucci, S., Vilella, A., & Gotti, C. (2018). Neuronal and extraneuronal nicotinic acetylcholine receptors. *Current Neuropharmacology*, *16*(4), 338–349. https://doi.org/10.2174/1570159X15666170912110450

Zuschratter, W., & Scheich, H. (1990). Distribution of choline acetyltransferase and acetylcholinesterase in the vocal motor system of zebra finches. *Brain Research*, *513*(2), 193–201. https://doi.org/10.1016/0006-8993(90)90457-M

How to cite this article: Asogwa, N. C., Toji, N., He, Z., Shao, C., Shibata, Y., Tatsumoto, S., Ishikawa, H., Go, Y., & Wada, K. (2022). Nicotinic acetylcholine receptors in a songbird brain. *J Comp Neurol*, *530*, 1966–1991. https://doi.org/10.1002/cne.25314